


REVIEW

Open Access

A survey on control issues in renewable energy integration and microgrid



Faisal R. Badal^{1*} , Purnima Das², Subrata K. Sarker¹ and Sajal K. Das¹

Abstract

This paper describes the usefulness of renewable energy throughout the world to generate power. Renewable energy adds a remarkable scope in power system. Renewable energy sources act as the prime mover of a microgrid. The Microgrid is a small network of power system with distributed generation (DG) units connected in parallel. The integration challenges of renewable energy sources and the control of microgrid are described in this paper. The varied nature of DG system produces voltage and frequency deviation. The unknown nature of the load produces un-modeled dynamics. This un-modeled dynamic introduces measurable effects on the performance of the microgrid. This paper investigates the performance of the microgrid against different scenarios. The voltage of the microgrid is controlled by using different controllers and their results are also investigated. The performance of controllers is investigated using MATLAB/Simulink SimPowerSystems.

Keywords: Renewable energy, Integral challenges, Microgrid, Control process, Voltage control

1 Introduction

The use of energy is rapidly increasing due to the growing nature of world's population. The generation of energy becomes an important issue for the world. The use of renewable energy sources is a big trend to address the energy generation. Renewable energy is the energy which comes from resources that are naturally not depleted by use [1]. Most common renewable energy sources are water, wind, solar and bio-fuel or biomass. The traditional use of these energy sources includes power generation, heating, and transport fuels. Renewable energy sources are of interest because of their ability to sustain. This results in an alternative to the decrease of conventional energy sources such as coal, petrol and nuclear energy. Renewable energy sources are clean sources of energy that have a much lower environmental impact as compared to the conventional energy sources [2]. Access to energy is essential for the economic growth of a country. In a typical developing country, every 1% growth of the GDP leads to a rise of 1.4% demand of electricity [3].

The demand of energy is expected to grow by almost forty percent by 2035 with an average of 1.4 percent in

each year and the demand for oil will increase by around 0.8 percent each year to 2035 [3, 4]. However the world holds only a reserve 40 years of supply of oil. Therefore the use of renewable energy sources is in high demand for next two decades or future. These renewable sources contribute 16% of global energy consumption with 10% coming from the traditional biomass which is mainly used for heating, 3.4% from hydroelectricity and rest of resources cover 2.6% [4].

Renewable energy replaces conventional fuels in four distinct areas: electricity generation, hot water/space heating, motor fuels, and rural (off-grid) energy services [5]. The main factors for developing renewable energies are able to lead a number of the positive results. Renewable energy sources are capable of controlling the greenhouse effect and climate change [6, 7]. In the area of space heating and transportation, the biogenetic fuel plays an appreciable function that verifies sustainable energy [7].

In 2016, the generation of worldwide electric power from various energy, including renewable energy sources is reported in Fig. 1 [8–10]. Figure 1 shows that the oil contributes 3% of total energy, while gas 43%, coal 4%, nuclear energy 25% and renewable energy 25%. The protection of electric energy from renewable energy sources plays a vital role in global energy supply. In 2016, the top countries that produced energy from renewable sources were Germany

*Correspondence: faisalrahman1312@gmail.com

¹Department of Mechatronics Engineering, Rajshahi University of Engineering and Technology, Kajla Rajshahi-6204, Bangladesh

Full list of author information is available at the end of the article

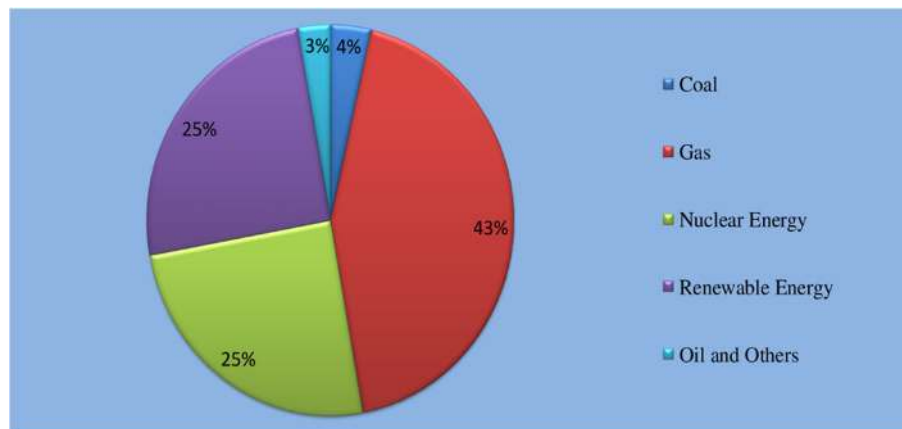


Fig. 1 Percentage of Electric Power Produced from Various Energy Sources in 2016 [8, 10]

(1,05,839 MW), China (5,45,206 MW), Japan (71,809 MW), Italy (51,485 MW), United States (2,14,766 MW), France (44,666 MW), Spain (47,954 MW), UK (33,544 MW), Australia (18,091 MW), Belgium (6696 MW), Thailand (8650 MW), Netherlands (7122 MW), Switzerland (15,195 MW) [8, 9, 11]. The fraction of renewable energy is presented in Fig. 2 that signifies the condition of the generation rate of energy from renewable energy sources in past, present and future.

Wind energy is the most promising renewable energy source. In 2016, the top wind energy generation countries that produced energy from wind turbine were China (1,68,690 MW), USA (82,184 MW), Germany (50,018 MW), India (28,700 MW), Spain (23,074 MW), UK (14,543 MW), France (12,066 MW), Canada (11,900 MW), Brazil (10,740 MW), Italy (9257 MW), Poland (5807 MW), Australia (4327 MW), Netherland (4206 MW), Japan (3234 MW), Austria (2632 MW) [8, 10].

Solar energy is the cleanest renewable energy source. In 2016, the top photovoltaic countries that produced

energy from solar were Germany (40,988 MW), China (77,434 MW), Japan (41,600 MW), Italy (19,251 MW), United States (34,711 MW), France (6767 MW), Spain (7171 MW), UK (11,250 MW), Australia (5632 MW), Belgium (3292 MW), Thailand (2154 MW), Netherlands (1955 MW), Switzerland (1644 MW) [8, 10].

Bioenergy is the another renewable energy source that plays an important role for producing energy. In 2016, the top bioenergy generation countries that produced energy from biomass were USA (12,458 MW), China (12,140 MW), Germany (9336 MW), UK (4993 MW), Japan (4076 MW), Italy (3833 MW), Thailand (3446 MW), France (1474 MW), Austria (1432 MW) [8, 10].

The photovoltaic panels and wind turbines are used as promising power source of microgrid to produce electricity. The generation of energy from the microgrid depends on solar strength and wind speed and produces some challenging criteria which are related to control technology of the microgrid [12]. Therefore, the management and reliability of the microgrid exposes research area to control

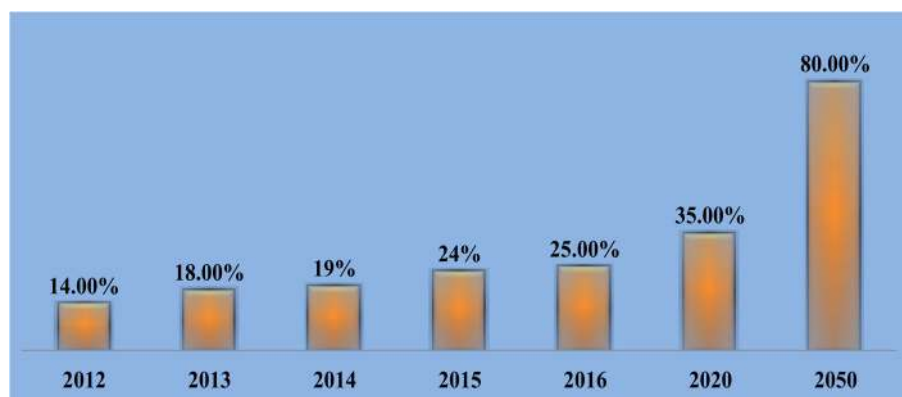


Fig. 2 Increasing Rate of Energy Generation from Renewable Energy Sources in Present and Future [8, 41]

engineers. The aim of this paper is to present a survey on integration and control issues of renewable energy. This paper also presents the control technology of the micro-grid and distributed regulated voltage supply with the inclusion of different types of load.

2 Renewable energy sources

A renewable electricity generation technology harnesses a naturally existing energy flux and converts that flux into electricity. It must be located at the place where natural energy flux is available to occur. This technology is differed from the conventional fossil-fuel and nuclear electricity generation. Unlike conventional fossil-fuel and nuclear electricity generation, this technology has no fuel cost.

2.1 Wind turbine

Wind energy is one of the most useful renewable energy sources to produce electricity [13–15]. The wind industry is rapidly increasing due to its faster turbine technologies, fresh technology for power system. A global statistic of wind generation from 2008 to 2016 is presented in Fig. 3 [8, 16, 17]. This statistic is the evidence of the increasing interest of wind turbine.

Wind generator uses either induction motor or synchronous motor [18]. Induction motors are widely used due to small in size, light in weight, easy to maintain. To describe the mathematical model of a wind generator, the following contains the required variable definitions [19–24]:

E_k = Kinematic energy (J);

P_w = Power (W);

m = Mass (Kg);

v_w = Speed of wind (m/s);

ρ = Density (Kg/m³);

A_s = Swept area (m²);

ζ = Speed ratio;

α = Pitch angle of blade (deg);

r = Radius of wind turbine (m);

ω_w = Angular velocity of wind turbine (rad/s);

$\frac{dm}{dt}$ = Mass flow rate of wind.

The kinematic energy produced by the blade of the wind turbine due to rotation is,

$$E_k = \frac{1}{2}mv_w^2 \quad (1)$$

The power of the wind generation is equal the rate of change of energy,

$$P_w = \frac{dE_k}{dt}$$

$$P_w = \frac{1}{2}v_w^2 \frac{dm}{dt} \quad (2)$$

Mass flow rate can be represented by

$$\frac{dm}{dt} = \rho A_s v_w \quad (3)$$

The power of the wind turbine can be defined by

$$P_w = \frac{1}{2}\rho A_s v_w^3 \quad (4)$$

The total available wind power can be represented by,

$$P_T = \frac{1}{2}\rho C_p \zeta A v_w^3 \quad (5)$$

Where,

$$\zeta = \frac{\omega_w r}{V_w}$$

$$C_p = 0.5(\vartheta - 0.022\alpha^2 - 5.6)e^{-0.17\vartheta}$$

And

$$\vartheta = \frac{3600r}{1609\zeta}$$

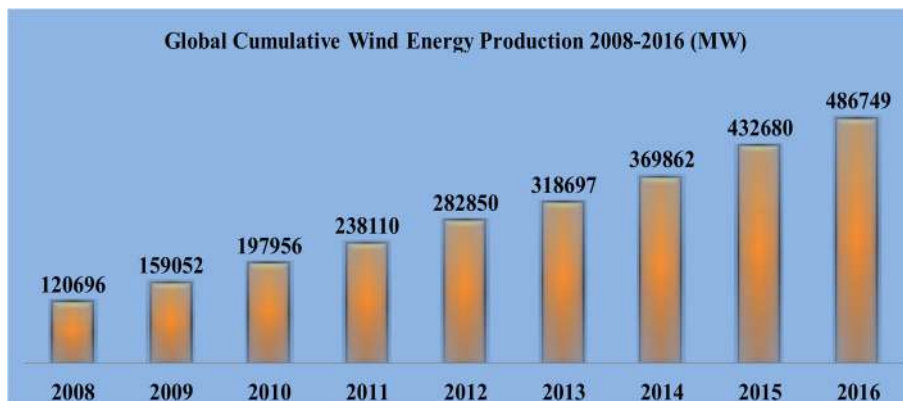


Fig. 3 Global Cumulative Wind Energy Generation in 2008-2016 [8, 17]

2.2 Solar system

Photovoltaic (PV) energy system decreases the demand of fossil fuels and acts as a clean and reliable renewable energy source [25]. Figure 4 [8, 26] represents the statistical improvement of the use of solar energy throughout the world [8, 13, 17].

The conversion of energy for the PV takes place using two methods. Photovoltaic is the direct method of producing electricity using photovoltaic effects [27–30]. Due to the variation of sunlight intensity, DC current is fluctuated in the photovoltaic system. This fluctuation is reduced by using inverter that supplies desired voltage and current. Concentrated solar power system is the indirect method which uses mirrors or lenses to produce electric current [31]. In this process a steam-driven turbine is used to convert the heat of the sun radiation [32–34]. The following table defines the variables to describe the mathematical model of the a system,

I_{pc} = Photo current (A);

I_{sc} = Short circuit current (A);

I_{cc} = Short circuit current of the solar cell (A);

I_{sr} = Irradiation of solar (W/m^2);

I_{ms} = Module saturation current;

T = Actual cell temperature;

T_{rc} = Cell temperature at reference condition;

R_{sr} = Intrinsic shunt resistance (Ω);

R_s = Series resistance (Ω);

Q = Charge of electron;

V_{oc} = Open circuit voltage (V);

N_{cs} = Cell number connected in series;

N_{cp} = Cell number connected in parallel;

N = Ideality factor of the diode in the circuit;

K = Boltzmann's constant = $1.38 \times 10^{23} J/K$;

ε_{be} = Energy of material band-gap.

An equivalent circuit of solar cell having PV arrays can be represented as shown in Fig. 5 [35, 36]. In PV array, the value of R_{sr} is kept very large while the R_s is kept very small to simplify the analysis of the solar system.

The module photo-current I_{pc} of the solar cell can be represented by,

$$I_{pc} = \frac{[I_{sc} + I_{cc}(T - 298)] * I_{sr}}{1000} \quad (6)$$

The Module reverse saturation current I_{rsc} is defined by,

$$I_{rsc} = \frac{I_{sc}}{\exp(Q * V_{oc}/N_{cs}KNT) - 1} \quad (7)$$

With the variation of cell temperature, I_{ms} can be represented as,

$$I_{ms} = I_{rsc} \left[\frac{T}{T_{rc}} \right]^3 \exp \left[\frac{Q * \varepsilon_{be}}{NK} \left(\frac{1}{T} - \frac{1}{T_{rc}} \right) \right] \quad (8)$$

The photovoltaic module having output current I ,

$$I = (N_{cp}I_{pc} - N_{cp}I_{ms}) * \left[\exp \left(\frac{V/N_{cs} + IR_s/N_{cp}}{NV_{dt}} \right) - 1 \right] - I_{rc} \quad (9)$$

Where, the thermal voltage of diode V_{dt} can be defined by,

$$V_{dt} = \frac{K * T}{Q}$$

and, Current through shunt resistance I_{rc} is,

$$I_{rc} = \frac{VN_{cp}/N_{cs} + IR_s}{R_{sr}}$$

2.3 Biomass

Biomass is another form of renewable energy that produces electricity with low cost, high capability and prevent global warming [37, 38]. It includes human and animal wastes, agricultural residues, growth plants, crops and algae [39]. A statistical report of the production of electricity from biogas is represented in Fig. 6 [8, 40, 41]. Biogas consists of different gases such as carbon-dioxide (25-45%), methane (50-75%), water vapor (2-8%) and many other gases namely nitrogen N_2 , oxygen O_2 , ammonia NH_3 etc. [42–44].

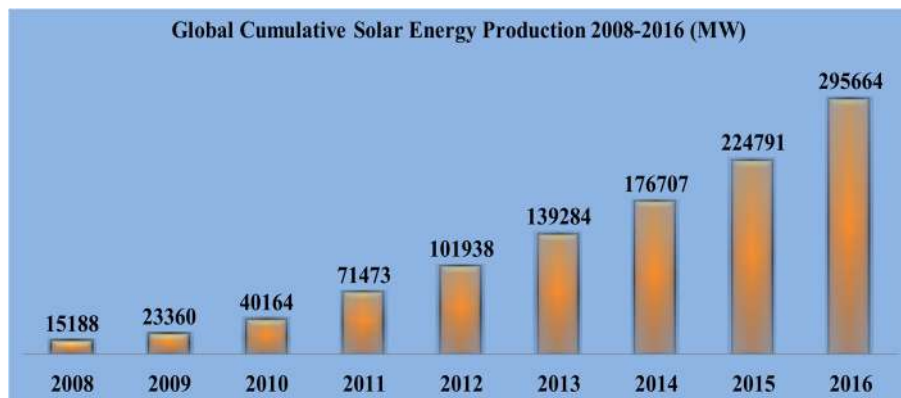


Fig. 4 Global Cumulative Solar Energy Generation in 2008-2016 [8, 26]

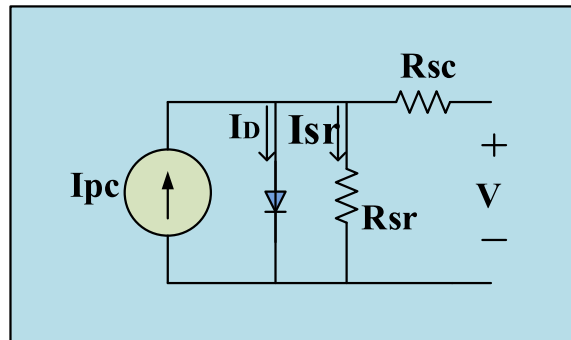
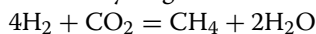


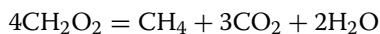
Fig. 5 Equivalent Circuit of Solar Cell. [5]

Figure 7 represents the basic block diagram for producing biogas using anaerobic digestion process that produces methane from agro-wastes or crops [45, 46]. The Anaerobic digestion of biomass consists of four steps, namely hydrolysis, acidogenesis, acetogenesis and methanogenesis [45]. Hydrolysis converts complex polymers into simple monomers and produces acetate and hydrogen. Carbon-dioxide and hydrogen sulfide are made by using ammonia through acidogenesis. Acetogenesis is used to digest these using acetate oxidizing bacteria. The last step is methanogenesis which produces methane, carbon-dioxide and water [47]. The basic reactions to produce methane using methanogenesis are represented:

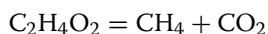
1. From hydrogen



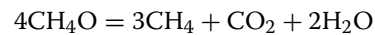
2. From Formate



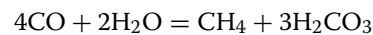
3. From acetate



4. From methanol



5. From Carbon monoxide



3 Electricity production method

3.1 Wind

Figure 8 represents a basic block diagram to produce electricity using wind turbine. It consists of two or three propeller or blade at the top of the turbine around a shaft. The wind circulation creates force on the shaft to rotate the rotor of the generator which produces electromagnetic induction. The flux across the conductor is changed to produce electricity. Two types of propeller are used in the wind turbine, namely drag type and lift type [48–51]. The drag type propeller has higher torque and slow rotating speed. Horizontal Axis Wind Turbine (HAWT) uses lift type propeller. Lower air pressure is created on the leading edge while higher air pressure is created at the tail edge.

Induction generator consumes more reactive power. To overcome this problem, double fed induction generator

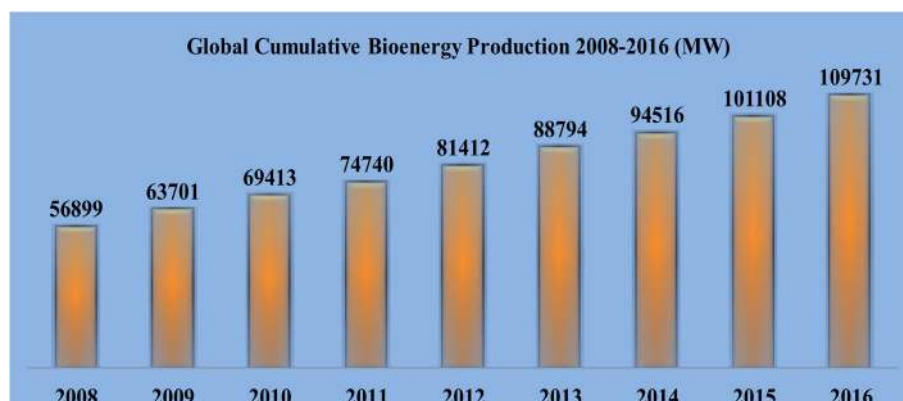


Fig. 6 Global Cumulative Bio-Energy Generation in 2008-2016 [8, 41]

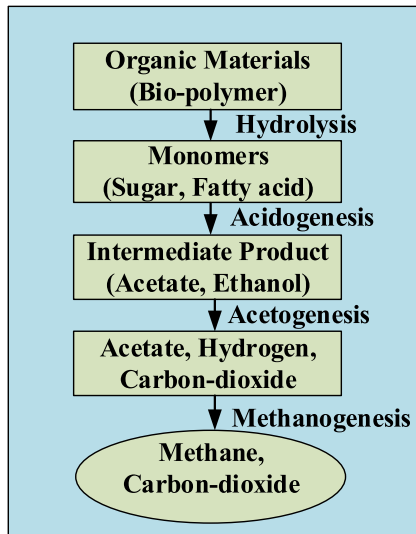


Fig. 7 Flow Chart of Methanogenesis Process

(DFIG) is widely used [52–55]. An inverter is used that controls the torque and real and reactive power of the machine by controlling the current.

3.2 Solar

A basic block diagram to produce electricity using solar system is represented in Fig. 9. Solar system consists of solar cells that convert the light energy into electricity [56–58]. When the photons of the sunlight hit the solar cell, it absorbs the photons. The energy of these photons conducts the electrons into the cell. If the energy of these photons is high enough to free the electrons, they carry the charge through the circuit.

The current produced by the solar system is known as light-generated current [59]. The photons absorbed by

the solar cell produce electron-hole pairs [60, 61]. The carriers are collected by using a p-n junction to separate the electron and hole. When the minority carriers reach to the p-n junction, it is swept by the electric field. By connecting the emitter and base together, the light generated by carriers flows through the external circuit.

3.3 Biomass

There are several methods to produce electricity from biomass. Figure 10 represents the production process of electricity using biogas. It includes a direct combustion of biomass using biogas. It produces heat which is used to heat the water to convert it into steam [39]. The steam is used to run a turbine to produce electricity. A second method where the biomass is gasified for producing useable gas [39, 62, 63]. In this process, a gasifier is used to take both dry and wet biomass. The dry biomass such as agricultural waste produces synthesis gas (CO + H₂) by high temperature in the absence of oxygen. Again wet biomass namely food waste is converted into methane (CH₄) gas. A gas turbine in this case can be fed by both synthesis and methane gas for electricity production.

4 Integration challenges

One of the major factors while connecting renewable energy sources to the main grid is that the electric grid must adapt the generation units. Different kinds of technical and economical challenges may be introduced while integrating renewable energy sources to the main grid [64].

The production of electricity from the solar panel is almost predictable. The electricity production depends on the light available and the time duration of the day, which are well known [65–67]. We know about the movement of the sun. But it becomes un-predictable with the presence

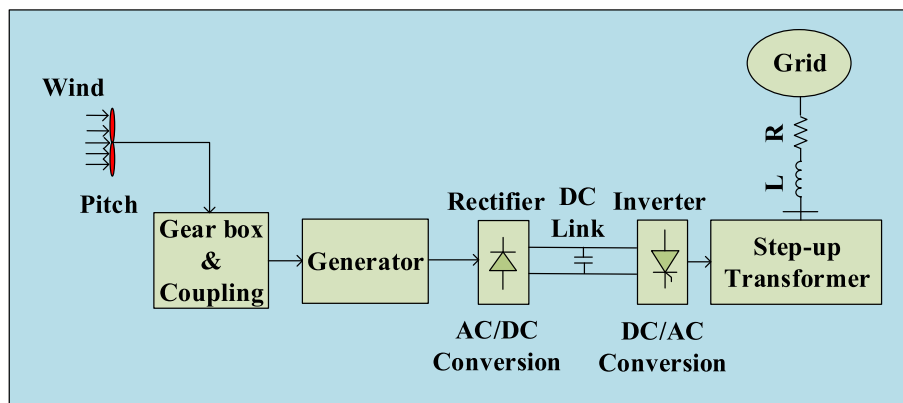


Fig. 8 Wind Energy Generation Process

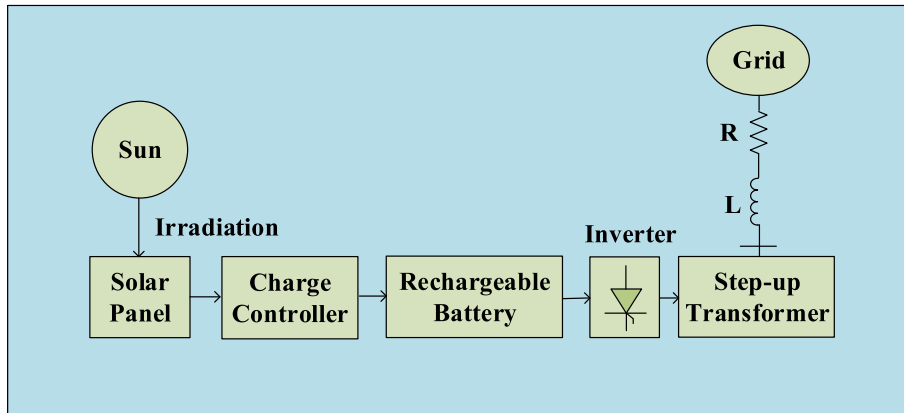


Fig. 9 Solar Energy Generation Process

of the cloud on the solar panel. Due to the cloud, enough light can not fall on the solar panel, which reduces the production of the electricity. Rain is the other drawback for the production of the electricity from the solar system. Again the generation of electricity is correlated with the daily condition, seasonal condition and the characteristics of the area. These uncertainties and variability of the solar system produce a challenge to control the main grid. This requires an additional technique to control the system. Again little adaptation is required for installing a small solar PV. But with the increasing of solar panel, the adaptation increases and thus, increases the cost and complexity. Distributed solar plants do not provide real-time generation data which make the operation complex. Voltage oscillation has an impact on the solar generation.

Wind generation is less predictable as compared to the solar system [65, 66]. The wind turbine is placed in an isolated and remote area from the main grid. This increases the economic cost and transmission losses. If the voltage loss is not calculated properly, the load voltage would be low. The motion of the wind is not constant over the day or season. The wind blows strongly at night and in the winter. When the production is excess than the demand, the current flow in the opposite direction which reduces the protection of the loads. To solve these problems, an extra control is required to step down the voltage [68]. Capacitor banks are used which store the electric power and inject the reactive power into the main grid. The load current is decreased which increases the load voltage. Any variation of the wind produces fluctuation of the voltage. This fluctuation can not be solved

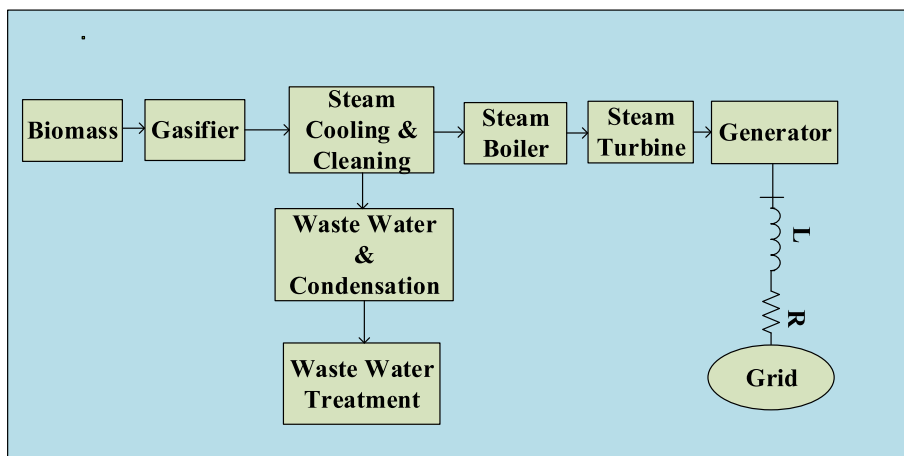


Fig. 10 Bio-Energy Generation Process

by the capacitor bank alone. It is replaced by a static var compensator (SVR).

The production of the electricity from biomass experiences some challenge during its operation. Gas production, gas cleaning, per-treatment etc. are the problems associated with biomass production [69]. The region of biomass production is mostly far from the power generation units. This increases the production cost of electricity. This long transportation also affects the property of biomass by introducing moisture and reducing bulk density. Though the moisture contained by the biomass that acts as a gasifying agent, excessive moisture becomes a challenge to control the production of electricity. Excessive Moisture presented in the biomass reduces the thermal efficiency by absorbing heat. The biomass should content a proper amount of moisture with it because dry biomass increases the production cost as it requires additional water to balance the production gas [70]. Excessive moisture is dried by the sunlight as well as the heat of the plant. Biomass drying process using sunlight is a long time process and depends on humidity. The drying process using heat of the plant is costly compared to the sunlight. These challenges vary the production rate of biogas. Thus the electricity produced by the gas turbine is not fixed. Those variations produce voltage fluctuation in the microgrid.

Voltage fluctuation, flickers, instability are introduced in microgrid with the variable nature of DG units [71]. It effects the dynamic and transient responses. The integration problem of DG units effects the active and reactive power and produces a sudden large change in power. The voltage may be oscillated due to harmonic injected into the system. The variable nature of DG units requires different power electronics device such as converter, filter which inject harmonic in microgrid. A fixed performance of DG units does not require the power converter. Thus, the harmonic distortion is controlled to a desired level. The reactive power of microgrid is consumed by the induction motor used in wind turbine as well as in the turbine used in biogas production. This consumption of reactive power produces voltage fluctuation at the point of common coupling (PCC).

A large number of DG units are connected to the microgrid. The connection between them should be proper for a better performance of microgrid. The power electronics that connect the microgrid and DG units are used to control the maximum power transfer. [14, 72–74]. The main task of power electronics is to pick up the maximum power from the sources and protects it from load dynamics [71]. The power transfer may be limited during a fault. Power electronics also control the power quality and active and reactive power on the grid side. It controls the frequency and eliminates the harmonic

from the system. The power converter controls the voltage of microgrid where microgrid is configured into two loops. The inner loop is called current controller in which power converter controls the power quality by controlling current. Power electronics control the active and reactive power to maintain the flow of power in the outer loop. The outer loop is called voltage controller that controls the grid voltage and increases the stability of the system. Synchronization methods such as phase-locked loop (PLL), zero-crossing method etc. are used to control the active and reactive power. Different kinds of energy storage systems such as batteries, flywheel, super-capacitor are used to improve the fault introduced in the system.

Microgrid with small-scale DG units are more expensive. Microgrid is made by a number of DG units grouped together [50]. Controls of these units make the system more complex. A proper communication system between the DG units is required to control the voltage and current of microgrid. Number of control techniques have been proposed to control the performance of microgrid. H_∞ is an optimal controller has been proposed to ensure robust performance of microgrid against different uncertainties [75–77]. The controller is designed based on H_∞ norms minimization. This control approach provides better performance with the fixed loading condition. Any perturbation of load hampers the stability of this controller.

Servomechanism controller has been applied to obtain robust performance of microgrid against different load uncertainties [78]. This control strategy is designed based on linear time invariant (LTI) theory. This control approach is able to control the variation of load parameters and ensures robust and stable performance with load parameter uncertainties. The performance of this controller is hampered by nonlinear load. Again, designing this controller for high order system is difficult and required advanced digital signal processing system.

To control the line voltage of microgrid, Non-linear feedback linearization controller is proposed [79, 80]. It controls the active and reactive power of microgrid to control the performance of the system. This control approach is designed by minimizing the nonlinearities of the system to make it a reduced order linear system. The performance of this controller is reduced by the unknown behavior of load and generators.

The motivation this paper is to present a survey on integration and control of renewable energy sources in microgrid. This paper also presents the technical challenges to control the performance of microgrid and control technology to control these challenges.

5 Microgrid

The demand for electric power is increasing day by day with the development of the world. Huge amount of natural assets such as fossil fuel, coal, natural gas, oil etc. known as nonrenewable source are used to produce electricity to satisfy the demand of electric power. It took million of time to form. But the natural assets are limited in the world. One day they will be finished and once we use up these nonrenewable sources, they will be gone for good which will be a great threat in the production of electricity. To solve this problem, researchers are interested to introduce new techniques which are enabled to satisfy the demand of the electricity with the development of the world. Microgrid is the reliable and more useful technique to produce electric power and reduce the use of the nonrenewable energy source. Microgrid (MG) is a small network of the main grid which is enable to produce electricity when it is disconnected from the main grid [81].

Microgrid can enable local electricity, energy storage, loads etc. to operate independently from the macrogrid [82]. During the interruption of the power flow of the main grid or when the main grid is unavailable, microgrid has an ability to operate locally. It must need sufficient capacity to fulfil the load requirements. Higher utilization of renewable energy sources, higher reliability, flexibility, power quality and sustainability, low capital investment, easy to operate, make it popular throughout the world [2].

Figure 11 represents the microgrid schematic. Microgrid consists of several components, namely distributed generation (DG), especially renewable energy sources (RES), point of common coupling (PCC), energy storage, voltage source inverter (VSI) [83, 84]. DGs units such as wind turbine, solar system, photovoltaic system, biomass, hydroelectric energy sources, fuel cell etc. are small sources of energy located near or at the point of

use. The energy provided by the DG units is DC. It requires a VSI unit to convert the DC power into AC power by using rectifier and inverter or only by inverter. Sometimes it also uses filter to stabilize the voltage and current. Both voltage and frequency can be converted by VSI units. Energy storage is used when generation units and loads are not at the same point. It can store and provide energy according to the requirement of the loads. It stabilizes the DG units output, provides a ride-through capability in the case of variation of the power of the sun, wind etc., provides backup power. Battery, flywheel, super-capacitor are used as the energy storage element. The connection between microgrid and main grid is called PCC. In the case of islanded microgrid, it is absent.

Microgrid can be connected to or disconnected from the main grid. According the connection, it is basically two types, namely Grid-connected mode and Island-connected mode [85]. In the grid-connected mode, there is a direct connection between the main grid and microgrid. Voltage and frequency is controlled by the main grid and microgrid acts as a constant power source. Due to the connection in a remote place, large amount of voltage drop is occurred. Voltage collapse, low power quality, large investment, huge transmission loss are the drawbacks of the grid-connected microgrid [86]. All these reasons, a microgrid is controlled in island-connected mode.

Voltage and frequency of the microgrid in islanded mode does not depend on the main grid. They can be controlled independently [87–91]. Wind turbine, solar system, biomass and many other renewable energy sources act as a prime mover of microgrid. They produce electric power and feed it to the microgrid. The performance of the microgrid directly depends on these renewable energy sources. The performance of the renewable energy sources depends on many factors such



Fig. 11 An Illustration of Islanded Microgrid Scheme

as wind, solar capacity and strength, sunlight etc. All these factors are not remaining constant for all the time. They vary with the variation of season, time. With the variation of these factors, the performance of these renewable energy sources is affected. Thus, the performance of microgrid is also changed [92]. Any change of these factors produces voltage and frequency oscillation and the operation of microgrid will be unsafe [93].

Different kinds of load dynamics or uncertainties hamper the achievement of microgrid and make the voltage of microgrid unstable. When the system is affected by these uncertainties, they will be unable to produce 50 Hz voltage and the voltage will be oscillated for a certain time [94]. Again with the increase of renewable energy source, the system becomes quite complex and produces many technical problems. As a result the performance such as steady state or transient response may be affected. It can also produce short circuit or malfunctions as well as reduce the power quality. The first and foremost requirement is to control the voltage of microgrid and make its performance reliable and stable.

5.1 Single phase microgrid modeling

The equivalent circuit of single phase microgrid is shown in Fig. 12a. Figure 13a represents the closed-loop configuration of single phase microgrid. A single phase microgrid consists of DC voltage source and many power electronics components that act as an interface between renewable energy sources and microgrid. Power electronics switch such as voltage source inverter (VSI) is used to convert the DC voltage into AC voltage and control the action of microgrid [95]. Insulated gate bipolar transistor (IGBT) is commonly used as VSI unit having faster switching speed. The switching speed of IGBT can be represented by $V_{sw} = \alpha(s)V_{dc}$ where V_{dc} is used to represent the DC voltage source [94]. Distributed generation (DG) units

such as wind turbine, solar system, biomass etc. produce electricity and control the active and reactive power. The power produced by these DG units is DC which is converted by AC power by VSI in such way that the total power of both DC side and AC side will be equal. Switching ripple having high frequency is feeble by using an LC filter.

The voltage across the inductor of the single phase microgrid can be represented by,

$$V_L = L \frac{dI_L}{dt} \quad (10)$$

if V_{sw} is the switching voltage of microgrid then,

$$\frac{dI_L}{dt} = \frac{V_L}{L} = \frac{V_{sw} - V_g}{L} \quad (11)$$

where I_L is the current through the inductor and V_g is the voltage across the capacitor which acts as a microgrid voltage. The Laplace transform of the Eq. (10) is

$$V_L(s) = sLI_L(s)$$

$$I_L(s) = \frac{V_L(s)}{sL} = \frac{V_{sw}(s) - V_g(s)}{sL}$$

The switching voltage V_{sw} is defined as the product of duty ratio of VSI and the supply dc voltage V_{dc} .

$$V_{sw} = \alpha(s)V_{dc}(s)$$

The grid voltage of single phase microgrid can be represented by,

$$C \frac{dV_g}{dt} = I_c$$

Here, I_c represents the current through the capacitor. By arranging this equation,

$$\frac{dV_g}{dt} = \frac{1}{C} I_c \quad (12)$$

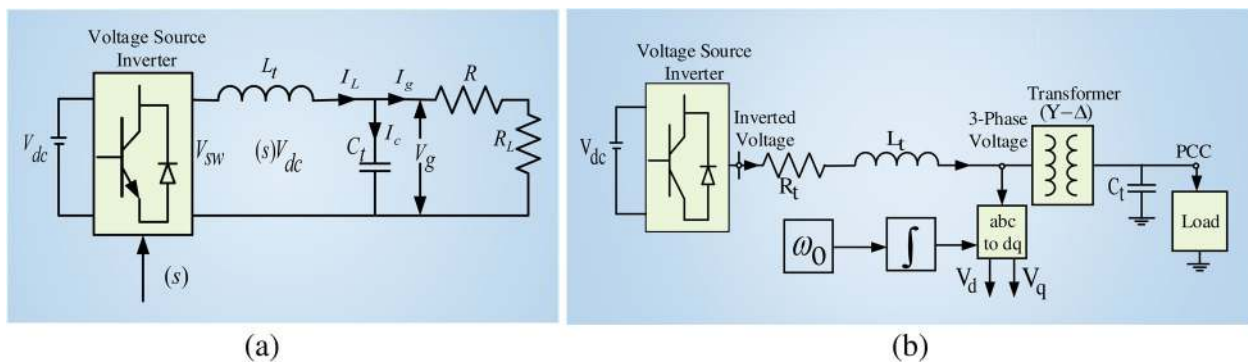


Fig. 12 (a) Single Phase Single Energy Source Microgrid System, (b) Three Phase Single Energy Source Microgrid System

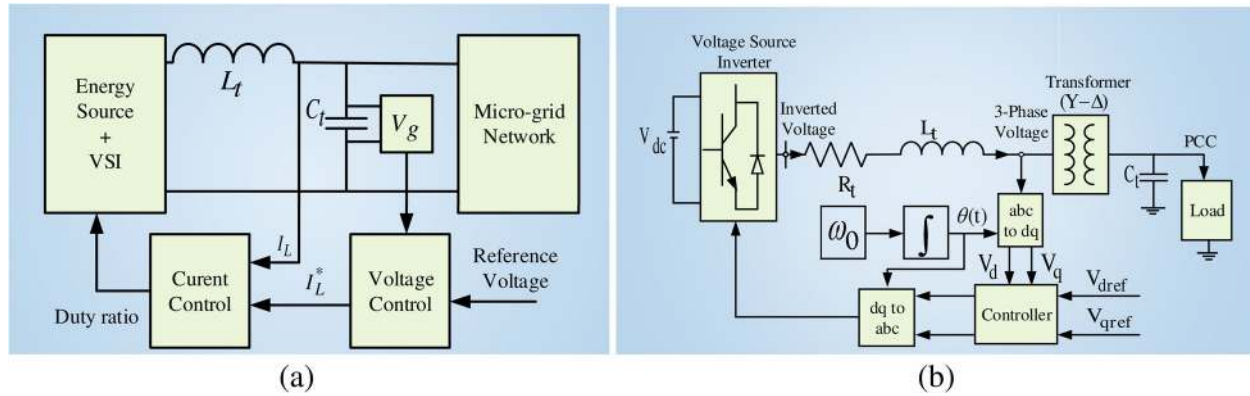


Fig. 13 (a) Closed-Loop Control Strategy in Single Phase Microgrid with VSI, (b) Closed-Loop Control Strategy in Three Phase Microgrid with VSI

For a linear time invariant system the state space equation may be defined as,

$$\frac{dx}{dt} = Ax + Bu \quad (13)$$

$$y = Cx + Du \quad (14)$$

where,

x = State matrix,

u = System input,

A = System matrix,

B = Control matrix,

C = Output matrix,

D = Transient matrix,

y = Output vector,

By comparing Eq. (11) and (12), the state matrix $x = \begin{bmatrix} I_L \\ V_g \end{bmatrix}$;

input variable $u = [V_{sw}]$ and the disturbance matrix $d = [I_g]$.

According to (13) and (14)

$$\frac{d}{dt} \begin{bmatrix} I_L \\ V_g \end{bmatrix} = \begin{bmatrix} 0 & -\frac{1}{L} \\ \frac{1}{C} & 0 \end{bmatrix} \begin{bmatrix} I_L \\ V_g \end{bmatrix} + \begin{bmatrix} I_L \\ 0 \end{bmatrix} [V_{sw}] + \begin{bmatrix} 0 \\ -\frac{1}{C} \end{bmatrix} [I_g]$$

and the output of the system can be represented by,

$$y = [V_g] = [0 \ 1] \begin{bmatrix} I_L \\ V_g \end{bmatrix}.$$

5.2 Three Phase Microgrid Modeling

A three phase equivalent circuit for islanded microgrid is shown in Fig. 12b. Figure 13b represents the closed-loop configuration of three phase microgrid with VSI [82, 96, 97]. The terminal voltage of VSI $\bar{V}_{t,abc}$ may be represented by,

$$\bar{V}_{t,abc} = L_t \frac{d\bar{I}_{t,abc}}{dt} + R_t \bar{I}_{t,abc} + \bar{V}_{abc} \quad (15)$$

The current through the inductor L_t is written by,

$$\bar{I}_{t,abc} = C_t \frac{d\bar{V}_{abc}}{dt} \quad (16)$$

For simplifying the analysis of three phase microgrid, the Eqs. (15) and (16) are converted into dq frame,

$$\frac{d\bar{I}_{t,dq}}{dt} + j\omega_0 \bar{I}_{t,dq} = -\frac{R_t}{L_t} \bar{I}_{t,dq} + \frac{1}{L_t} \bar{V}_{t,dq} - \frac{1}{L_t} \bar{V}_{dq} \quad (17)$$

$$\frac{d\bar{V}_{dq}}{dt} + j\omega_0 \bar{V}_{dq} = \frac{1}{C_t} \bar{I}_{t,dq} \quad (18)$$

Now using (13) and (14) we consider $G_M(s) = C_M(s\bar{I} - A_M)^{-1}B_M + D_M$, where

$$A_M = \begin{bmatrix} 0 & \omega_0 & \frac{1}{C_t} & 0 \\ -\omega_0 & 0 & 0 & \frac{1}{C_t} \\ -\frac{1}{L_t} & 0 & -\frac{R_t}{L_t} & \omega_0 \\ 0 & -\frac{1}{L_t} & \omega_0 & -\frac{R_t}{L_t} \end{bmatrix}$$

$$B_M = \begin{bmatrix} 0 & 0 \\ 0 & 0 \\ \frac{1}{L_t} & 0 \\ 0 & \frac{1}{L_t} \end{bmatrix}, C_M = \begin{bmatrix} 1 & 0 & 0 & 0 \\ 0 & 1 & 0 & 0 \end{bmatrix} \text{ and } D_M = 0$$

Where the state vector $x = [\bar{V}_d \ \bar{V}_q \ \bar{I}_{td} \ \bar{I}_{tq}]^T$; input vector $u = [\bar{V}_{td} \ \bar{V}_{tq}]^T$ and the output vector $y = [\bar{V}_d \ \bar{V}_q]$.

6 Microgrid control

6.1 Centralized control

The art to control of a flexible microgrid in both grid-connected mode and islanded mode, the knowledge of architecture of the system, system planning, and the topologies related to microgrid are necessary. Fault monitoring and protection of the microgrid is an important issue. The interconnection of different electronics, energy storage system, telecommunication makes the system complex.

Different kind of control methods are available for microgrid. Centralized control method is one of them [98]. Centralized controller is based on hierarchical control method. A hierarchical system has three control element, namely [99, 100], i) Local microsource controller (MC) with load controller (LC); ii) Microgrid central controller (MGCC); iii) Distributed management system (DMS). In a centralized controller, a central controller gathers information from all units. This central controller is the backbone of the system which performs all the calculation and produces control action for all units connected at a single point.

Local microsource controller (MC) is used to control the power electronics interface without communication system of the distributed generator connected to the microgrid [100, 101]. It has three elements, namely voltage source inverter (VSI), prime mover and DC interface. The VSI unit controls the amplitude and the phase of the output voltage. It also controls the active and reactive power of microgrid. MC takes the local information from the units [102]. Using these information, it controls the voltage and frequency of the microgrid. When it is connected to the power grid, it follows the information from the central controller. The load controller at the controllable load controls the load of the microgrid.

Microgrid central controller (MGCC) acts as an interface between distributed management system and microgrid [103]. It estimates the power amount for the microgrid drawn from the DG units. It produces a control signal which is sent to both MC and LC to optimize the electricity [99]. The order of the MGCC is carried by the MCs and LCs during grid connected mode while they have own control during islanded mode. Distributed management system (DMS) is also known as distribution network operator (DNO) [99]. It controls the operation of low and medium voltage areas.

6.2 Decentralized control

Decentralized control approach is hierarchical control in which each unit has a local controller [98, 104]. These units are controlled independently by its own local controller. The local controller receives local information and produces control action to maintain the local units. The controllers do not depend on the control of other controller's action. A strong coupling is required between the units of the system.

A decentralized control is fully opposite of the centralized control approach. In decentralized control, MCs are responsible to compete the maximize production to fulfil the demand [105]. It maximizes the autonomy of the micro-sources and loads. One of the advantages of decentralized control approach is, it uses different intelligent process. The control process of decentralized control

is based on peer-to-peer algorithm such as multi-agent algorithm, gossip-based algorithm [106, 107].

A decentralized control approach has the following characteristics for microgrid [106, 108];

1. Micro-source consists of different owners and each decision is taken locally.
2. The controller of each unit in the microgrid works based on intelligent algorithm.
3. Local micro-source supplies power to the distribution networks as well as produces heat for local installation, provides a backup power in case of emergency. It also keeps the voltage at a certain level.

The main advantage of the decentralized control is that it can embody different DG units with the microgrid without any change of the controller settings. But in this case, the coordination must be enough strong. The energy management system (EMS) of decentralized control approach is highly feasible [109]. The energy storage system (ESS), used as a voltage source, is controlled by either constant current mode or constant voltage mode. The state of charge (SOC) is adjusted by the ESS itself during the operation in constant current mode [108]. The EMS receives the information from SOC and produces control action to the DG units. Then the DG units maintain the value of SOC. [109].

The main disadvantage of the decentralized control is that, when the ESS is used as a voltage source, it is suffered by the lack of SOC information for the DG units [109]. There is no communication system is used in decentralized control method. Thus, the SOC information is not transferred to dispatchable DG units and for this reason the ESS is not stable.

In centralized approach, extensive communication and computation is required in an extended geographic area. This requirement makes the centralized control approach infeasible. Again, it is also not possible to make a fully decentralized control approach because it requires a very strong coupling between the operation of the units. The local variables are unable to supply minimum level of coordination of the units in the system. To solve these problems, hierarchical control approach is divided into three levels, namely primary, secondary and tertiary level shown in Fig. 14 [98].

The primary control level is usually droop control which shares the load between the converters in microgrid. On the other hand, the secondary control level reduces the steady-state error which is produced by the droop control and the tertiary level are responsible to export or import energy for microgrid.

6.3 Primary control

The first level of hierarchical control is primary control approach also known as internal or local control [98]. It is based on the local measurement. Output and

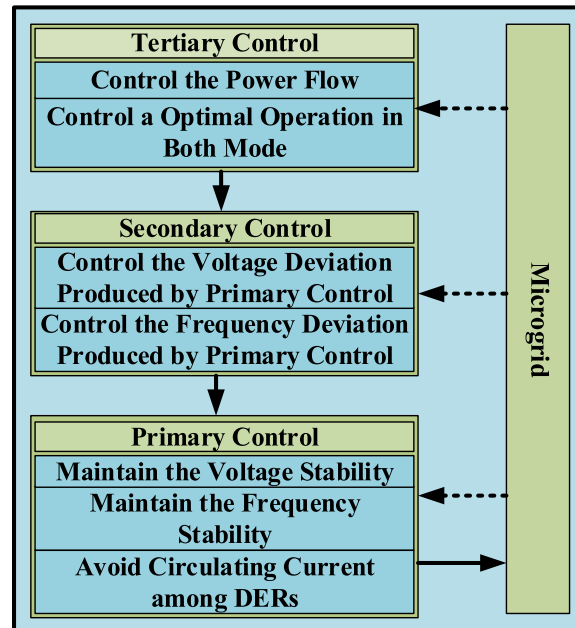


Fig. 14 Block Diagram of Hierarchical Control System

power sharing control is the main aim of this control. Primary control approach controls the voltage and frequency of the reference voltage that is fed to the inner current and voltage-control loops. It also controls the active and reactive power without any communication link and improves the power reliability [110–113]. Over-current in the power electronics device can damage the DC link capacitor. This control approach reduces the circulating current that may produce over current.

Primary controller counterfeits the behaviour of synchronous generator in which voltage regulator controls the power sharing. Since renewable energy sources produce DC voltage which is converted to AC voltage for the further process. This conversion is done using voltage source inverter (VSI) which fixes the frequency and voltage of the microgrid. It can provide distributed power generation system and make the voltage stable [112]. It does not need the requirement of external reference to stable and control the power. VSI can also be used in grid-connected mode, where the voltage source is converted by current source. To control the frequency and inertia of synchronous machine, VSI controller provides two functions such as i) control of DC power sharing and ii) control of inverter output [72, 111, 112, 114]. The DC power sharing controller controls the sharing of active and reactive power and reduces the mismatch in microgrid. This is done by using active power-frequency droop controller as well as reactive power-voltage droop controller. Inverter output controller regulates the output voltage and current using outer voltage and inner current loop.

VSI are connected in parallel in the microgrid that improve the performance and stability of microgrid by adjusting voltage and frequency using P/Q droop control method [115–118]. The droop control method can be expressed as:

$$f = \bar{f} - m(P - \bar{P}) \quad (19)$$

$$V = \bar{V} - n(Q - \bar{Q}) \quad (20)$$

Where \bar{f} and \bar{V} are frequency and amplitude of output voltage, f and V are reference frequency and voltage, P is active power, \bar{P} is active power reference, Q is reactive power, \bar{Q} is reactive power reference, m and n are Corresponding slope. The parameter m and n can be designed as follows to synchronise the system as well as stable the voltage:

$$m = \frac{\delta f}{P_{max}}$$

$$n = \frac{\delta V}{2Q_{max}}$$

Where P_{max} and Q_{max} are the maximum allowed active and reactive power, δf and δV are maximum allowed

frequency and voltage. But if the inverter absorbed the active power, then the slope m can be written as

$$m = \frac{\delta f}{2P_{max}}$$

When the droop control method used in large power system, the output and line impedance of the synchronous machine is inductive [115]. Then the output voltage and frequency depends on an impedance angle ϕ and can be described as:

$$f = \bar{f} - m[(P - \bar{P})\sin\phi - (Q - \bar{Q})\cos\phi] \quad (21)$$

$$V = \bar{V} - n[(P - \bar{P})\cos\phi + (Q - \bar{Q})\sin\phi] \quad (22)$$

Beside outer voltage and inner current loop, primary control approach also has virtual output impedance loop. The outer voltage loop controls the output voltage whereas the inner current loop controls inductor or capacitor current. Virtual output impedance loop provides proper output impedance. This control technique increases the durability of the parameter and the output voltage \bar{v}_0 can be expressed as:

$$\bar{v}_0 = v_{ref} - Z_v i_0 \quad (23)$$

Where Z_v virtual output impedance and v_{ref} is the voltage reference expressed by

$$v_{ref} = V\sin(2\pi ft)$$

The virtual impedance is mainly kept bigger than the value of output impedance of the inverter plus the line impedance. Thus, the equivalent output impedance is governed by the virtual output impedance and it has no power loss. The resistance can be implemented with no efficiency loss [117, 118].

6.4 Secondary control

Secondary control level is also known as energy management system (EMS) that supervises the system and collects information from the DG units for regulating the microgrid. It is preferable for both grid-connected and islanded mode with reliable and secure operation. The main function of EMS is to find the optimal unit commitment (UC). The primary control level produces some voltage and frequency deviation which is compensated by the secondary control level [119]. It has three option such as i) real-time optimization, ii) expert system and iii) decentralized hierarchical control to find the despatch and unit commitment of the microgrid [120]. The supervisory

system sends a signal through low-bandwidth communication to regulate the voltage to an optimal value. It also synchronizes the microgrid with the main grid before the interconnection departing from islanded mode to grid-connected mode.

The secondary control level can operate in stand-alone mode. The time frame of this control approach is slower than the primary control approach. Thus, the secondary control is easily decoupled from the primary control level as well as it can reduce the bandwidth of the communication using microgrid variables [121]. Secondary control approach senses the frequency f_{mg} and amplitude V_{mg} and compares with the reference frequency \bar{f}_{mg} and reference amplitude \bar{V}_{mg} using compensator [115]. The compensator produces errors f_ϵ and V_ϵ which are send to the system to compensate the frequency and voltage deviation by restoring them. For a AC microgrid these errors can be expressed by:

$$f_\epsilon = k_{pf}(\bar{f}_{mg} - f_{mg}) + k_{if}(\bar{f}_{mg} - f_{mg})dt + \Delta f \quad (24)$$

$$V_\epsilon = k_{pv}(\bar{V}_{mg} - V_{mg}) + k_{iv}(\bar{V}_{mg} - V_{mg})dt \quad (25)$$

Where k_{pf} , k_{if} , k_{pv} and k_{iv} are control parameter of the compensator and Δf are synchronization term. The value of Δf is zero when the grid absent. The value of f_ϵ and V_ϵ must not cross the maximum frequency and voltage deviation.

6.5 Tertiary control

The highest level of hierarchical control is tertiary control approach [98]. It adjusts the set point of the inverters in the microgrid to control the power flow [116]. A system may have multiple microgrid interconnecting to each others. The coordination of the operation of these microgrid is selected by the tertiary control level. It is also responsible to find the communication requirement from the main grid such as frequency regulation, voltage supports etc. Tertiary control approach sends information to the secondary control level that coordinates the primary control level and subsystems in the microgrid within a few minutes. After that, the primary controller can react instantaneously to the local events in a predefined way. Tertiary control approach also reduces voltage harmonic by harmonic injection.

Tertiary control level is mainly considered as a part of the main grid, not the microgrid itself [115, 122]. The active and reactive grid power P_g and Q_g is measured at the point of common coupling (PCC) and compared with the reference \bar{P}_g and \bar{Q}_g . Thus the reference frequency \bar{f}_{mg} and \bar{V}_{mg} voltage is expressed as follows:

$$\bar{f}_{mg} = k_p P(\bar{P}_g - P_g) + k_i P \int (\bar{P}_g - P_g) dt \quad (26)$$

Table 1 Parameter values for single phase microgrid

Description	Value
DC bus voltage (V_{dc})	300V
Capacitor filter (C_f)	15 μ F
Inductor filter (L_f)	2mH
Line resistance (R_{line})	0.45 Ω
Consumer load (R)	40 Ω

$$\bar{V}_{mg} = k_p Q(\bar{Q}_g - Q_g) + k_i Q \int (\bar{Q}_g - Q_g) dt \quad (27)$$

Where $k_p P$, $k_i P$, $k_p Q$ and $k_i Q$ are the control parameters of the compensator of tertiary control level. The reference frequency \bar{f}_{mg} and voltage \bar{V}_{mg} are generated by the secondary controls [123, 124]. The export and import of active and reactive power depends on the sign of \bar{P}_g and \bar{Q}_g . The power flow of the tertiary control approach is bidirectional. The grid frequency f_g and voltage V_g are constant.

The active and reactive power is controlled by adjusting reference frequency and voltage. The microgrid feeds P or Q to the main grid if $\bar{f}_{mg} > f_g$ or $\bar{V}_{mg} > V_g$ respectively. When the value of $k_i P$ and $k_i Q$ is equal to zero, the tertiary control approach can be considered as a primary controller which are responsible to interconnect multiple microgrid and improve power quality at the PCC.

7 Control methods

Voltage and frequency control is the main requirement of islanded microgrid. In the case of grid-connected mode, the voltage and frequency of microgrid are directly controlled by main grid. The main grid provides the required performance of microgrid. But when the microgrid is disconnected from the main grid, the grid has no impact on the performance of microgrid. As a result the voltage

Table 2 Parameter values for three phase microgrid

Description	Value
DC bus voltage (V_{dc})	2000V
VSC terminal voltage (line-line) (V_{base})	600V (1 pu)
Transformer voltage ratio (Y/Δ)	0.6/13.8
PWM carrier frequency (f_{sw})	1980 Hz
System frequency (f_0)	60 Hz
VSC filter resistance (R_f)	1.5m Ω
DG rated power (S_{base})	3MVA(1 pu)
VSC filter inductance (L_f)	100 μ H
VSC filter capacitance (C_f)	100 μ F
Load resistance (R)	4.33 Ω
Load capacitance (C)	100 mH
Load inductance (L)	1 pF

and frequency may be deviated due to many reasons. The performance of islanded microgrid largely depends on the physical environment. Unpredictable uncertainties and unknown load dynamics can deviate the performance of microgrid. Thus, it may unable to produce 50 Hz voltage during its operation. Again, the voltage and frequency may be unstable. To make the voltage and frequency stable in all modes of operation, a number of methods have been proposed in the technical literature.

7.1 Integral linear quadratic Gaussian controller

The integral linear quadratic gaussian (ILQG) controller has been proposed for tracking the performance of single phase islanded microgrid. This controller has large bandwidth as well as large gain and phase margin. It has the ability to track the reference single using H_2 norm which provides large gain of the controller. The design of LQG controller without the action of integral part has lack of ability to make the system robust against different uncertainties produced by the environment [125]. The Integral controller alone is used to track the reference signal by reducing error [126]. Though this controller has large gain at low frequency, it provides a low performance against plant dynamics. The problems of LQG and integral controller are improved by designing integral LQG controller.

The ILQG controller is designed by assuming the state-space model of the plant. The design process is described for tracking control in the islanded MG system. Consider the following state-space model of the plant:

$$\dot{x}(t) = Ax(t) + Bu(t) + D\alpha(t), \quad (28)$$

$$y(t) = Cx(t) + \bar{D}\bar{\alpha}(t), \quad (29)$$

Where

x = State vector

y = Output of the plant

u = Input of the plant

A = System matrix

B = Input matrix

C = Output matrix

D and \bar{D} = Noise matrices of the system.

w = Process noise

\bar{w} = Measurement noise

A proper selection of the noise terms in these equations provides a reliable and robust performance. The robustness of the system is increased by reducing uncertainties as well as process and measurement noise by noise term D and \bar{D} . The controller is designed by minimizing quadratic cost function J ;

$$J = \lim_{T \rightarrow +\infty} \mathbf{E} \left[\frac{1}{T} \int_0^T (x(t)^T Q x(t) + u(t)^T R u(t)) dt \right]. \quad (30)$$

Here, Q and R are the symmetric weighting matrices where $Q \geq 0$ and $R > 0$ and E is the desired value. The desired performance of the controller is achieved by a proper choosing of Q and R matrix in the cost function (30).

The updated plant $P(s)$ with an integral controller of the plant can be represented by;

$$\bar{x}_f(t) = A_f x_f(t) + B_f u(t) + B_f \alpha_1, \quad (31)$$

$$z_f(t) = C_f x_f(t) + \beta. \quad (32)$$

With $A_f = \begin{bmatrix} A & 0 \\ C & 0 \end{bmatrix}$, $B_f = \begin{bmatrix} B \\ 0 \end{bmatrix}$, and $C_f = \begin{bmatrix} C & 0 \\ C & I \end{bmatrix}$. The augmented vector $x_f = [x \int y dt]^T$, $z_f = [z_1 \ z_2]^T$ and $\beta = [\alpha_2 \ \alpha_3]^T$. α_1 is defined as mechanical noise of the system, α_2 is the sensor noise from the output y and α_3 is the sensor noise which is added to the integral part.

The updated plant have the cost function for designing integral LQG controller;

$$J = \lim_{T \rightarrow +\infty} \mathbf{E} \frac{1}{T} \int_0^T [x^T Q x + w(y)^T \bar{Q} f(y) + u^T R u] dt, \quad (33)$$

Where $f(y)$ is the weighting matrices, Q is the state matrix, \bar{Q} is integral state matrix and R is control input matrix with $Q \geq 0$, $\bar{Q} \geq 0$, and $R > 0$.

The integral LQG controller is estimated by using kalman filter and linear quadratic regulator (LQR) controller. The state-space equation of ILQG controller is represented by;

$$\dot{\bar{x}}_f(t) = A_f \bar{x}_f(t) + B_f u(t) + K_1 (z_f - C_f \bar{x}_f), \quad (34)$$

$$u(t) = -K_2 \bar{x}_f. \quad (35)$$

With \bar{x}_f is augmented state vector. \bar{x}_f is defined by using kalman filter. K_1 is the kalman gain and K_2 is feedback gain matrix. The kalman gain K_1 can be represented by;

$$K_1 = P_1 C_f^T R_1^{-1}, \quad (36)$$

Where P_1 is the solution of algebraic riccati equation (ARE) which can be represented by;

$$\bar{P}_1 = A_f^T P_1 + P_1 A_f - P_1 C_f^T R_1^{-1} C_f P_1 + Q_1 \quad (37)$$

Where Q_1 is non-negative defined ($Q_1 \geq 0$) and R_1 is positive defined ($R_1 > 0$).

And feedback gain matrix K_2 can be represented as;

$$K_2 = R_C^{-1} B_f P_2, \quad (38)$$

P_2 is the solution of algebraic riccati equation which is represented by

$$\bar{P}_2 = A_f^T P_2 + P_2 A_f - P_2 C_f^T R_2^{-1} C_f P_2 + Q_2 \quad (39)$$

Where $Q_2 \geq 0$ and $R_2 > 0$. The control parameter Q_1 , R_1 , Q_2 and R_2 is adjusted properly for a better performance of the integral LQG controller.

7.2 Proportional integral derivative controller

Proportional Integral Derivative (PID) controller is the most widely implemented controller in different industries. This controller is easy to design and simple. Low order transfer matrices and simplicity makes this control algorithm popular. This control algorithm dose not require high level of knowledge. It minimizes the steady state error to improve the responses [127]. Parameters selection is an important task to improve the performance of PID controller. Root-locus, Ziegler-Nichols, Chien-Hrones-Reswick, Cohen-Coon and Wang-Juang-Chan are the useful tools to tune the parameters of the controller.

The transfer function of PID controller consisting of Proportional, Integral and Derivative structures in a single package is represented by

$$C(s) = K_p + \frac{K_i}{s} + K_d s = \frac{K_d s^2 + K_p s + K_i}{s}$$

Where K_p is the proportional gain, K_i is the integral gain and K_d is the derivative gain of PID controller. The transient response of the system is improved by proportional gain where the integral gain is responsible to minimize the steady-state error. The derivative gain of PID controller reduces the overshoot of the system.

Cohen-Coon is an important tool that tunes the parameters of PID controller efficiently [128]. This algorithm is well suited for a wide variety of process than the other algorithm. The output response of this algorithm is recorded based on Fig. 15. In Fig. 15, L is the delay time, T is time constant. This tuning method is a self regulation process that tunes the parameters of the PID controller directly.

$$K_p = \frac{1.35}{a} \left(1 + \frac{0.18\tau}{1 - \tau} \right), K_i = \frac{K_p(1 - 0.39\tau)}{L(2.5 - 2\tau)}$$

$$K_d = \frac{K_p L(0.37 - 0.37\tau)}{1 - 0.81\tau}$$

Where $a = kL/T$ and $\tau = L/(L + T)$.

The microgrid voltage fluctuates for connecting and disconnecting loads and different disturbance. The performance of PID controller using Cohen-Coon method is investigated against many scenarios such as harmonic loads (television, computer, printers), noise etc. It provides a robust voltage tracking against all disturbance.

7.3 Model predictive controller

Model predictive controller (MPC) has been proposed in this section to control the voltage of single phase islanded microgrid [129, 130]. It is an advanced method used in the process industries as well as power system to reduce the tracking error based on dynamic models of the process. MPC has the ability to predict the future events and can take control action accordingly. It can predict the change

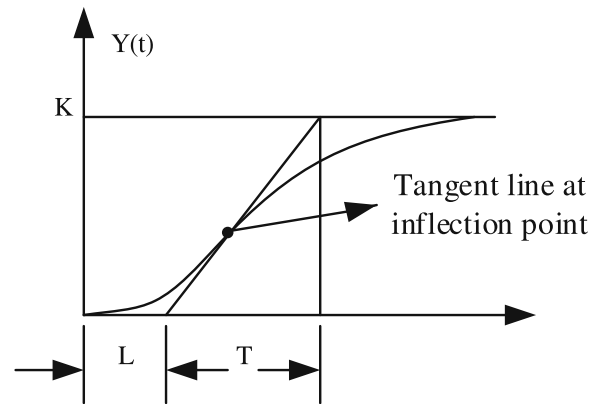


Fig. 15 Response curve of Cohen-Coon tuning formula

in the dependent variables caused by independent variables. MPC uses the current plant measurement, dynamic state, the process variable target to calculate the future events. This controller uses predefined cost function to calculate the optimal values of the future control inputs.

The state-space model to design the controller is represented as follows:

$$x_p(k+1) = A_p x_p(k) + B_p u(k) \quad (40)$$

$$y_p(k) = C_p x_p(k) + D_p u(k) \quad (41)$$

Where A_p , B_p , C_p and D_p represents the discrete state-spaces of plant model, u is the manipulated variable, y_p is the process output and x_p is the state variable vector. According to the principle of receding horizon control to predict and control the events of the plant a current information of the plant is required. The increments of the variable $x_p(k)$ and $u(k)$ is represented as follows:

$$\Delta x_p(k+1) = A_p \Delta x_p(k) + B_p \Delta u(k) \quad (42)$$

And

$$y_p(k+1) = C_p x_p(k+1) \quad (43)$$

The plant can be rearranged in the following way

$$\begin{bmatrix} \Delta x_p(k+1) \\ y_p(k+1) \end{bmatrix} = \begin{bmatrix} A_p & 0 \\ C_p A_p & I \end{bmatrix} \begin{bmatrix} \Delta x_p(k) \\ y_p(k) \end{bmatrix} + \begin{bmatrix} B_p \\ C_p B_p \end{bmatrix} \Delta u(k) \quad (44)$$

$$y_p(k) = [0 \ I] \begin{bmatrix} \Delta x_p(k) \\ y_p(k) \end{bmatrix} \quad (45)$$

Where

$$A = \begin{bmatrix} A_p & 0 \\ C_p A_p & I \end{bmatrix}, B = \begin{bmatrix} B_p \\ C_p B_p \end{bmatrix}, C = [0 \ I]$$

And

$$\Delta u(k) = u(k) - u(k-1)$$

$$\Delta x_p(k+1) = x_p(k+1) - x_p(k)$$

$$\Delta x_p(k) = x_p(k) - x_p(k-1)$$

The future state variables and output sequence can be denoted by

$$\begin{aligned} x_p(k+H_y|k) &= A^{H_y} x_p(k) + A^{H_y-1} B \Delta u(k) \\ &+ \dots + A^{H_y-H_c} B \Delta u(k+H_c-1) \end{aligned}$$

where H_y is prediction horizon, the length of optimization window and H_c is control horizon, detect the number of parameters which are used to measure the future control actions which is chosen to less than or equal to H_y . And

$$\begin{aligned} y_p(k+H_y|k) &= C A^{H_y} x_p(k) + C A^{H_y-1} B \Delta u(k) \\ &+ \dots + C A^{H_y-H_c} B \Delta u(k+H_c-1). \end{aligned}$$

Assuming that at the sampling instant k_j , where $k_j > 0$, the state $x_p(k_j)$ provides the current plant information. Thus, the future state variables can be calculated using a set of future control parameters:

$$\begin{aligned} x_p(k_j+1|k_j) &= A x_p(k_j) + B \Delta u(k_j) \\ x_p(k_j+2|k_j) &= A x_p(k_j+1|k_j) + B \Delta u(k_j+1) \\ &= A^2 x(k_j) + A B \Delta u(k_j) + B \Delta u(k_j+1) \end{aligned}$$

⋮

$$\begin{aligned} x_p(k_j+H_y+1|k_j) &= A^{H_y} x_p(k_j) + A^{H_y-1} B \Delta u(k_j) + \\ &A^{H_y-2} B \Delta u(k_j+1) + \dots + A^{H_y-H_c} B \Delta u \\ &(k_j+H_c-1) \end{aligned}$$

Hence, the periodic output variables can be written as

$$\begin{aligned} y_p(k_j + 1|k_j) &= CAx_p(k_j) + CB\Delta u(k_j) \\ y_p(k_j + 2|k_j) &= CA^2x_p(k_j) + CAB\Delta u(k_j) + CB \\ &\quad \Delta u(k_j + 1) \\ &\vdots \\ y_p(k_j + H_y + |k_j) &= CA^{H_y}x_p(k_j) + CA^{H_y-1}B\Delta u(k_j) + \\ &\quad CA^{H_y-2}B\Delta u(k_j + 1) + \dots + CA^{H_y-H_c} \\ &\quad B\Delta u(k_j + H_c - 1) \end{aligned}$$

The dimension of H_y is Y and H_c is Δu for the single input and single output case, then

$$\begin{aligned} Y &= [y_p(k_j + 1|k_j)y_p(k_j + 2|k_j)\dots y_p(k_j + H_y + |k_j)]^T \\ \Delta U &= [\Delta u(k_j)\Delta u(k_j + 1)\dots\Delta u(k_j + H_c - 1)]^T \end{aligned}$$

The prediction horizon can be arranged in a compact matrix form

$$Y = \alpha x(k_j) + \beta \Delta U$$

Here, the α matrix having dimension (H_y, n) and the β matrix having dimension (H_y, H_c) as follows:

$$\alpha = \begin{bmatrix} CA \\ CA^2 \\ CA^3 \\ \vdots \\ CA^{H_y} \end{bmatrix}$$

$$\beta = \begin{bmatrix} CB & 0 & \dots & 0 \\ CAB & CB & \dots & 0 \\ CA^2B & CAB & \dots & 0 \\ \vdots & \vdots & \vdots & \vdots \\ CA^{H_y-1}B & CA^{H_y-2}B & \dots & CA^{H_y-H_c}B \end{bmatrix}$$

The cost function C that reflects the control objective as

$$C = \sum Q(y_p(k_j + p|k_j) - R_p(k_j + p))^2 \sum R(\Delta u(k_j + p - 1))^2$$

where Q is the state weighting matrix, R_p is the reference signal and R is the control weighting matrix.

The constrained variable is parameterized using vector ΔU and expressed in a set of linear equation. The constraints are taken into consideration for each moving horizon window. This allows us to vary the constraints at the beginning of each optimization window, and also gives us the means to tackle the constrained control problem numerically. The constraints at sample time k_j are expressed as

$$\Delta u^{min} \leq \Delta u(k_j) \leq \Delta u^{max}$$

where u^{min} and u^{max} are the low and high levels of the control action respectively. The next constraints at future sample will be

$$\Delta u^{min} \leq \Delta u(k_j + 1) \leq \Delta u^{max}$$

The inequality constraints for the parameter vector ΔU that minimizes the cost function is

$$\begin{bmatrix} M_1 \\ M_2 \\ M_3 \end{bmatrix} \Delta U = \begin{bmatrix} N_1 \\ N_2 \\ N_3 \end{bmatrix} \quad (46)$$

Where N is the element of Δu^{min} and Δu^{max} and M is a matrix reflecting the constraints, having the rows equal to the number of constraints and columns equal to the dimension of ΔU .

Since the cost function C is a quadratic, and the constraints are linear inequalities, then an optimal solution is found for standard quadratic programming problem. The expression can be written as,

$$M\Delta U \leq \gamma; \gamma \in \mathbb{R}^{N*1}$$

The results of the this controller provide a tracking performance of the microgrid. This controller is tested against different disturbance namely harmonic load, non-linear load, dynamic load, unknown load etc. The results against these scenarios exhibit a reliable performance of this controller.

7.4 Damping controller

Damping controller is a renewed controller to control the grid voltage and current based on negative imaginary (NI) approach. This controller is designed for both single and three phase islanded microgrid. Based on different dynamic loads and uncertainties, the performance of the microgrid is investigated using this controller. NI system is one which has no pole in the right half plane and the nyquist plot has phase within $[-180,0]$ for all $\omega > 0$ where $j(G(j\omega) - \bar{G}(j\omega)) > 0$. This controller is easy to design and implement which does not require advanced digital signal processing.

The unwanted oscillation of voltage of single phase and three phase islanded microgrid is eliminated by this controller. Single phase islanded microgrid having the transfer function

$$C(s) = -k \frac{s^2 + 2\zeta\omega s}{s^2 + 2\zeta\omega s + \omega^2} \quad (47)$$

with k is the controller gain, $\omega > 0$ is the resonant frequency and $\zeta > 0$ is the damping constant where $k > 0$, $\omega > 0$ and $\zeta > 0$. The controller has zero at the origin, which indicates low gain with low frequency. Thus, it provides high gain margin and phase margin which increases the stability of the system. The controller ensures high performance based on the negative imaginary approach. A system is stable when the product of the loop gain

of a system has a value less than one and the system is strictly NI. The close-looped transfer function $G(s)$ can be represented as follow;

$$G(s) = \frac{G_s(s)}{1 - G_s(s) * C(s)}$$

where $G_s(s)$ is the plant transfer function and $C(s)$ is the controller transfer function.

This controller is also designed for three phase islanded microgrid. It is a great challenge to control the performance of three phase islanded microgrid because it consists of a number of subsystem. Each subsystem has DG units which need to control properly. This controller provides a robust performance of the three phase microgrid. The transfer function of three phase islanded microgrid is expressed by

$$C_m(s) = -k \frac{s^2 + 2\zeta\omega s}{s^2 + 2\zeta\omega s + \omega^2} \eta_{n*n} \quad (48)$$

With η_{n*n} is a square matrix of order n which indicate the number of input and output. Based on NI approach the result of islanded microgrid is investigated under different load conditions and uncertainties. The results prove the stability and high performance of the controller. The close-looped transfer function for three phase islanded microgrid is expressed by;

$$G_{Mcl}(s) = \frac{G_M(s)}{1 - G_M(s) * C_m(s)}$$

with $G_M(s)$ is the plant transfer function and $C_m(s)$ is the controller transfer function for three phase islandad microgrid.

8 Performance evaluation

The performance of the controllers is investigated in this section for different scenarios. The parameters value of single and three phase islanded microgrid are listed in Tables 1 and 2. The performance of the microgrid system against the unknown load dynamics, highly nonlinear and unbalanced loads are verified. The microgrid system is implemented in MATLAB to obtain the simulation results. The results show the effectiveness of controllers.

8.1 Performance evaluation for single phase single energy source microgrid

8.1.1 Performance against dynamic loads

An islanded microgrid is a small station of power separated from the main grid whose voltage and frequency control become a challenge. The performance of microgrid may be affected by the dynamic loads such as induction motor [131]. It reduces the stability and produces unreliable performance of microgrid. To investigate the performance of microgrid in the presence of dynamic load, A single phase dynamic load block is modeled as a current source with active power of 50 MW and reactive

power of 25 MW at initial voltage. Due to load dynamic, the system voltage is changed which affects the active and reactive power. The effect of short or open circuit produces fault current in the line. When a circuit is interrupted by some failures or disconnected that produces open circuit fault and stops the flow of current while short circuit fault produces large current flow through the load which can damage the load. The simulation results shown in Figs. 17b, 18b, 19b and 20b that ensure the tracking and reliable performance of the controllers.

8.1.2 Performance against harmonic loads

Television, computer, printers, fluorescent lighting, battery chargers, rectifiers etc. are the example of harmonic loads which are increasing with the development of the world [132]. The harmonic loads produce considerable voltage and current harmonic in the power system which unstable the performance of microgrid. The current waveform becomes quite complex due to the presence of harmonic load which increases excessive amount of current in the system. Harmonics in power systems increase heating in the equipment and conductors, misfiring in variable speed drives and produce unsafe operation of microgrid. Voltage harmonics are caused by current harmonics. The voltage provided by the voltage source will be distorted by current harmonics due to source impedance. This is particularly the case for the third harmonic in the system. To investigate the performance of the microgrid, a 3rd order harmonic current source is designed in Fig. 16b of amplitude 7A and frequency 150Hz with a 30Ω resistance is connected with the current source. These controllers reduce the voltage and current harmonics and ensures the robust performance of the controller shown in Figs. 17c, 18c, 19c and 20c.

8.1.3 Performance against unknown loads

The load which is not related to the model of microgrid is unknown load that influences the performance of microgrid [82]. Any un-modeled load can be introduced in the power system which vary the voltage and power. In this paper an unknown load is modeled in Fig. 16c which is connected in parallel with the microgrid. The un-modeled load is connected with the microgrid at $t= 0.3$ seconds when the switch is pressed, which changes the steady state of the microgrid and the resistance, inductance and capacitance are also changed. The peak amplitude of load voltage remains unchanged with the load change and the fault current is investigated in Figs. 17e, 18d, 19e and 20d which indicate the robustness and tracking performance of the controllers.

8.1.4 Performance against Asynchronous machine loads

Asynchronous machine load such as induction motor hampers the performance of microgrid and reduces

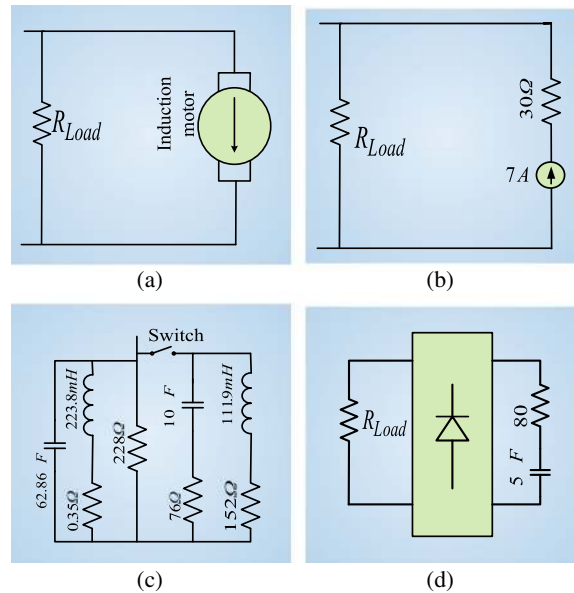


Fig. 16 Inclusion of (a) Asynchronous Machine Load, (b) Harmonic Load, (c) Unknown Load, (d) Non-linear Load with Microgrid

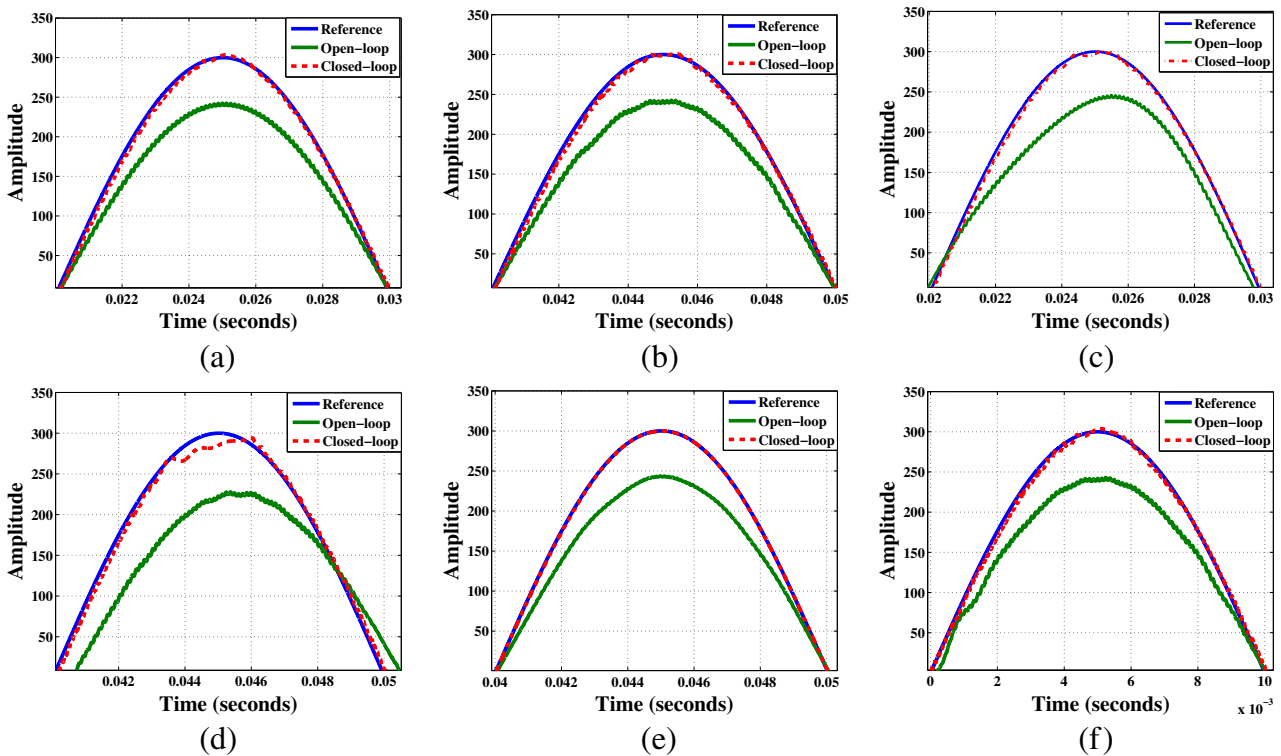


Fig. 17 Grid Voltage Tracking Using ILQG Controller for (a) Consumer Load, (b) Dynamic Load, (c) Harmonic Load (d) Asynchronous Machine Load, (e) Unknown Load, (f) Non-linear Load. The Blue (-) and Green (-) Solid Line Represents the Reference and Open-loop Voltage Respectively and Red (-) Dotted Line Represents the Closed-Loop Grid Voltage

the stability of the system [133]. To investigate the influence of the asynchronous load on microgrid, an induction motor is modeled in the dq stator reference frame shown in Fig. 16a, having a zero steady-state condition is paralleled with the microgrid. The performance of these controllers are investigated having capacitor-start and capacitor-start-run. Due to the presence of asynchronous machine load, the grid voltage may fluctuate which vary the active and reactive power of microgrid. These controllers reduce the fluctuation of voltage and provide most reliable performance of the microgrid system presented in Figs. 17d, 18e, 19d and 20e.

8.1.5 Performance against non-linear loads

The operation of microgrid is influenced by the highly non-linear load namely television, computer [134]. A non-linear load is modeled in Fig. 16d by two-phase four-pulse diode bridge rectifier connected to the PCC. The output terminal is connected to an RC load having $R = 80\Omega$ and $C = 5\mu\text{F}$. The input current of the rectifier may be distorted, but these controllers provide stable, reliable and high quality voltage investigated in Figs. 17f, 18f, 19f and 20f.

8.2 Performance evaluation for three phase single energy source microgrid

8.2.1 Performance against three phase non-linear load dynamics

The performance of three phase islanded microgrid against nonlinear load is investigated in this section [134]. A nonlinear load is modeled which is same as the load used in single phase microgrid. The three phase nonlinear load is modeled using six pulse diode-bridge rectifier. The result of three phase islanded microgrid against highly nonlinear load is investigated by connecting the load to the PCC for $t = 0.3\text{s}$ to 0.33s shown in Fig. 21c. This section shows the results of damping controller, which insure the high performance and robustness of this controller. Similar results are obtained by using the others controller.

8.2.2 Performance against three phase balanced and Unbalanced load conditions

This section presents the performance of three phase islanded microgrid against balanced and unbalanced load [134]. A resistive load with active power 3 kW and phase voltage 60V is added to microgrid between time $t = 0.15\text{s}$ to $t = 0.16\text{s}$ to make the load voltage balanced. The result

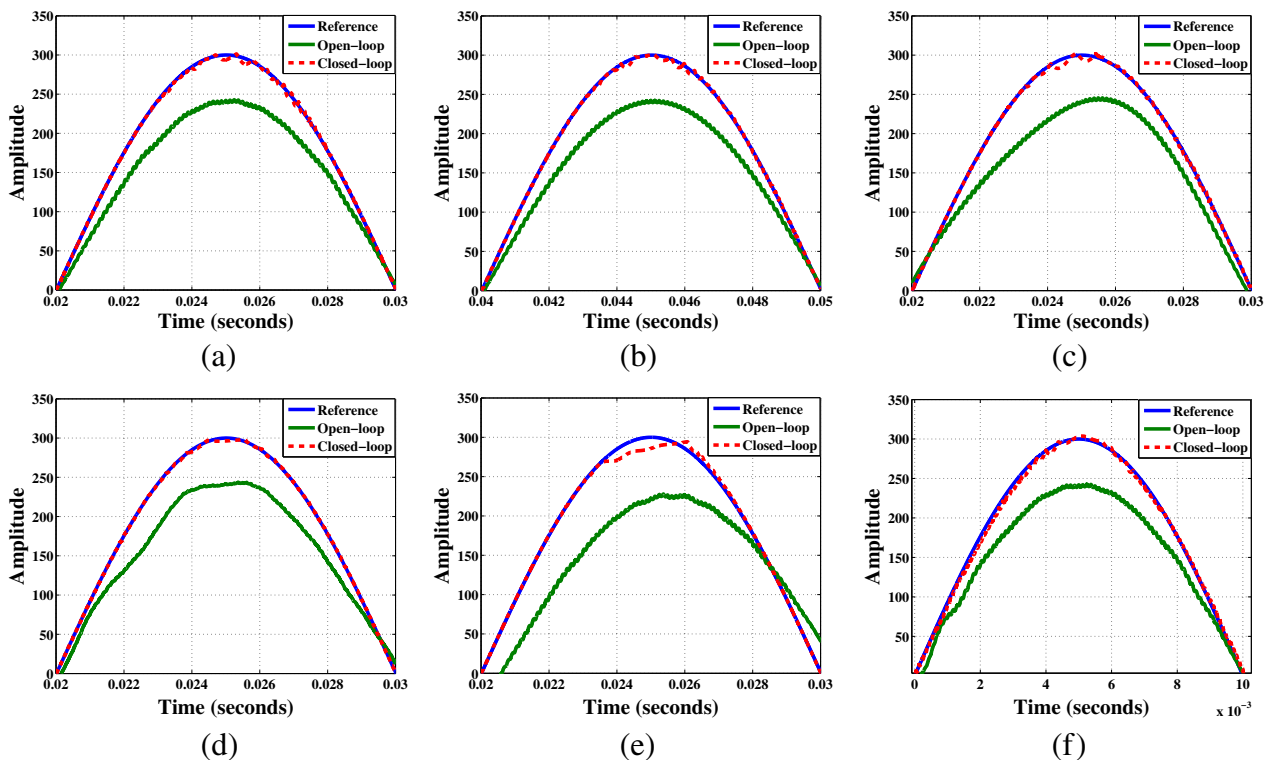


Fig. 18 Grid Voltage Tracking Using Model Predictive Controller for (a) Consumer Load, (b) Dynamic Load, (c) Harmonics Load, (d) Unknown Load, (e) Asynchronous Machine Load, (f) Non-linear Load. The Blue (-) and Green (-) Solid Line Represents the Reference and Open-Loop Voltage Respectively and Red (- -) Dashed Line Represents the Closed-Loop Grid Voltage

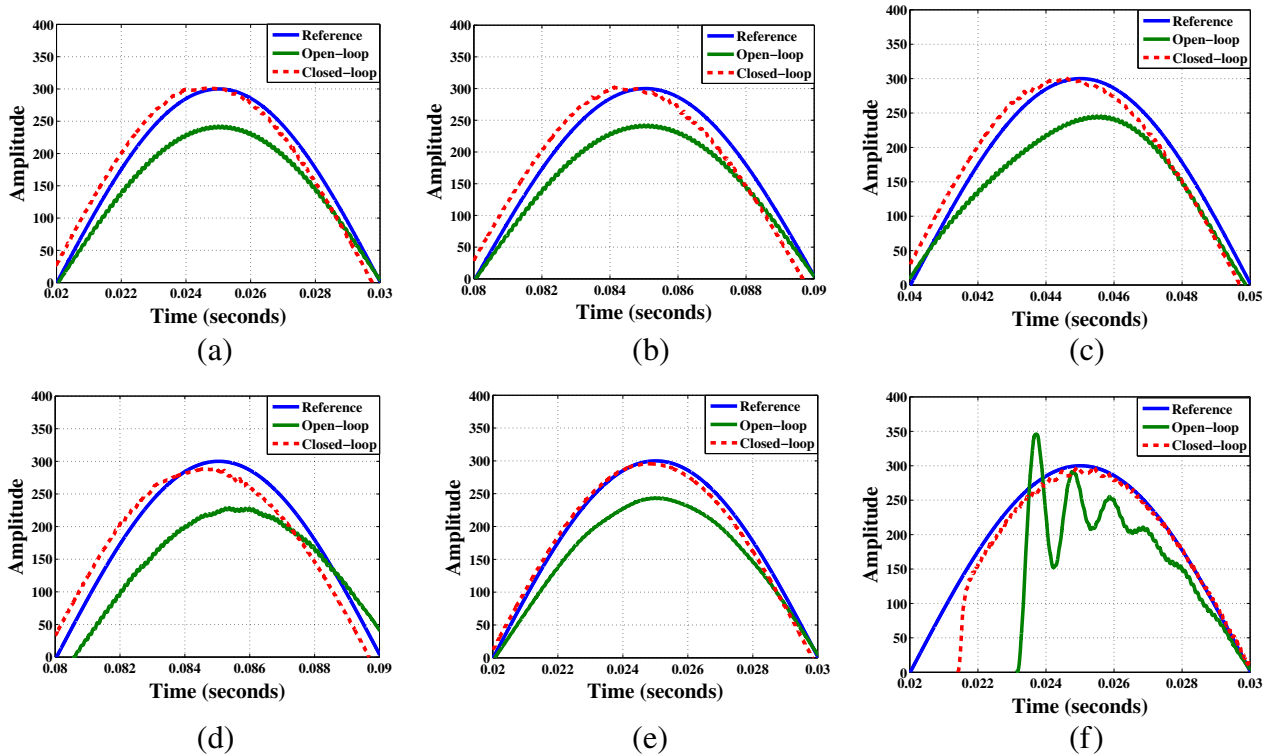


Fig. 19 Grid Voltage Tracking Using Damping Controller Under (a) Consumer Load, (b) Dynamic Load, (c) Harmonic Load, (d) Asynchronous Machine Load, (e) Unknown Load model, (f) Non-linear Load. The Green (-) and Blue (-) Solid Line Represents Response of $G_s(s)$ and Reference Signal Respectively, While Red (-) Dashed Line Represents the Response of $G(s)$

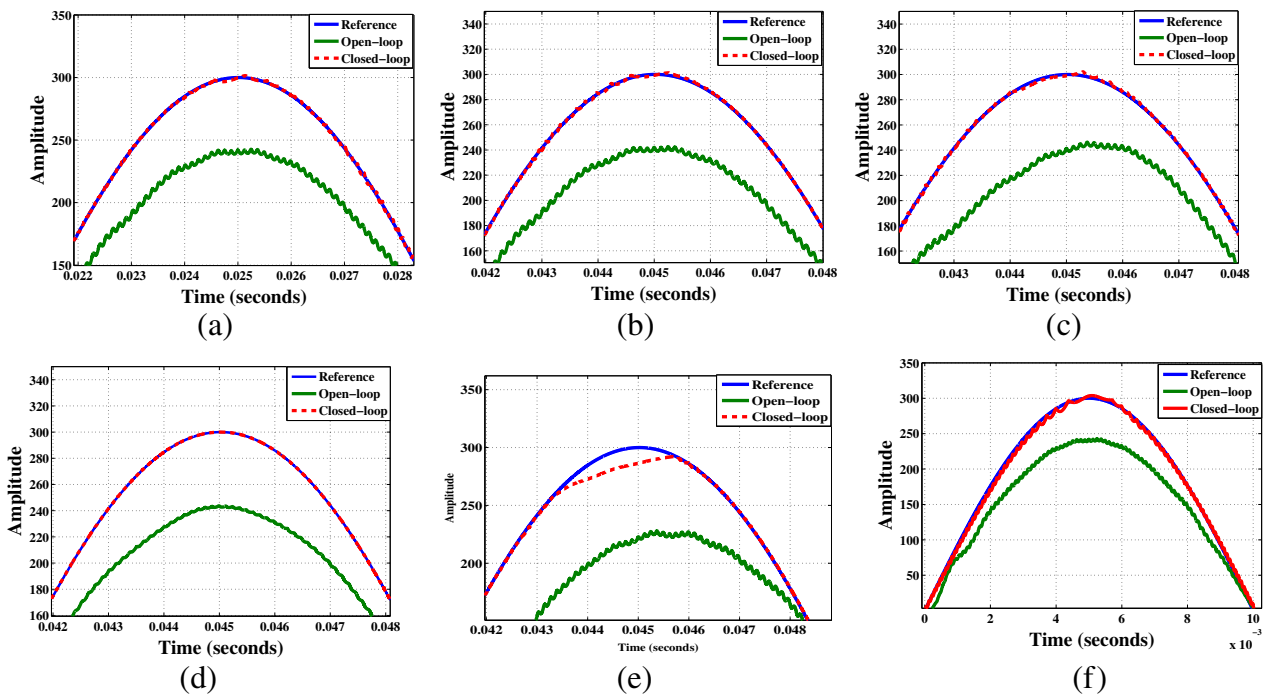


Fig. 20 Grid Voltage Tracking Using PID Controller for (a) Consumer Load, (b) Dynamic Load, (c) Harmonics Load, (d) Unknown Load, (e) Asynchronous Machine Load, (f) Non-linear Load. The Blue (-) and Green (-) Solid Line Represents the Reference and Open-Loop Voltage Respectively and Red (-) Dashed Line Represents the Closed-Loop Grid Voltage

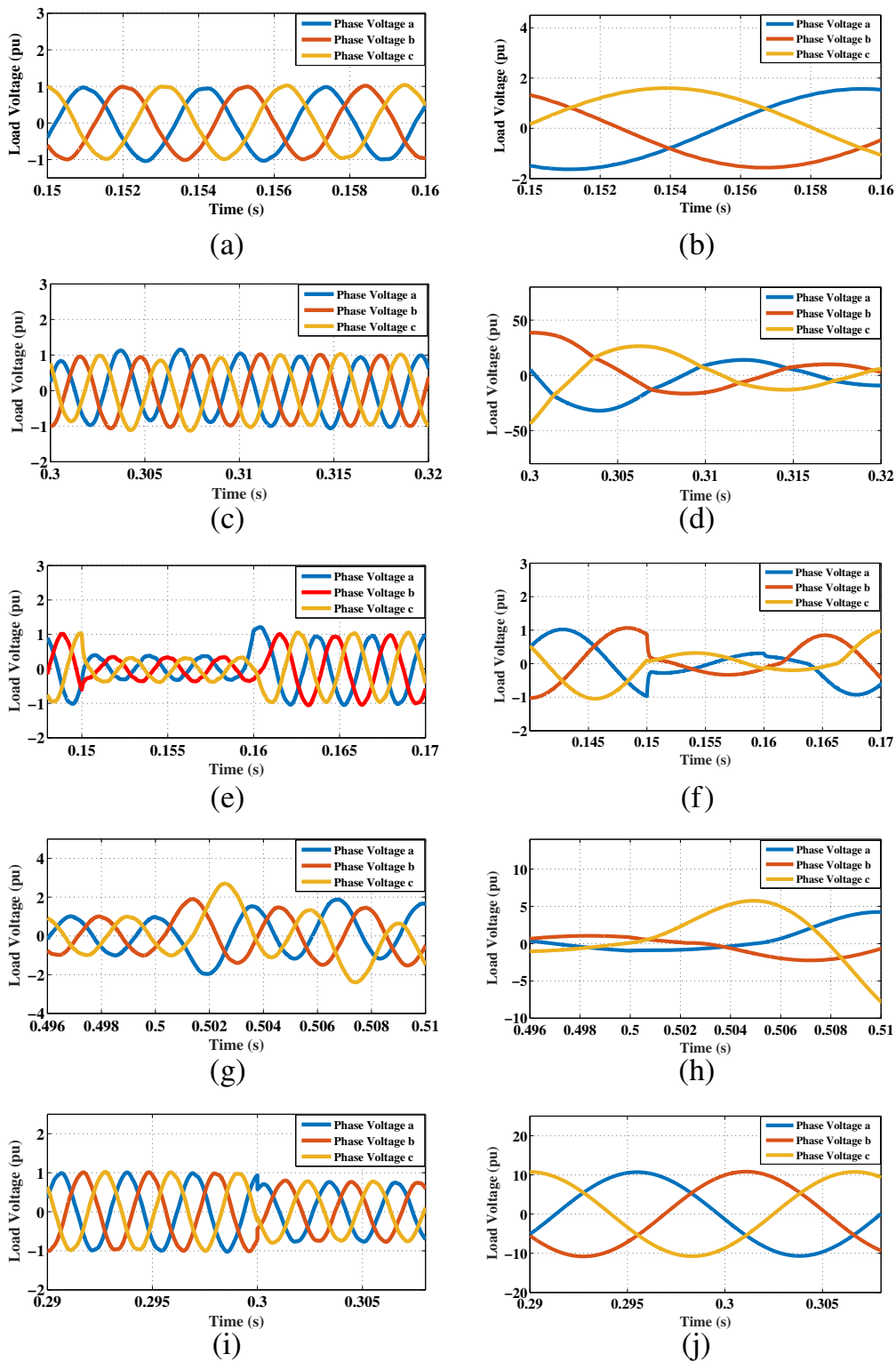


Fig. 21 Comparison of Load Voltage $V_{abc}(s)$ between $G_M(s)$ and $G_{Mcl}(s)$ Using Damping controller Under Different Loads, **(a)** Load Voltage of $G_{Mcl}(s)$ When Using Consumer Load, **(b)** Load Voltage of $G_M(s)$ When Using Consumer Load, **(c)** Load Voltage of $G_{Mcl}(s)$ When Using Non-linear Load, **(d)** Load Voltage of $G_M(s)$ When Using Non-linear Load, **(e)** Load Voltage of $G_{Mcl}(s)$ When Using Balanced Load, **(f)** Load Voltage of $G_M(s)$ When Using Balanced Load, **(g)** Load Voltage of $G_{Mcl}(s)$ When Using Unbalanced Load **(h)** Load Voltage of $G_M(s)$ When Using Unbalanced Load, **(i)** Load Voltage of $G_{Mcl}(s)$ When Using Unknown Load and **(j)** Load Voltage of $G_M(s)$ When Using Unknown Load

shown in Fig. 21e ensures that the damping controller balances the load voltage to a desired voltage. An unbalanced load is connected to the PCC after $t = 0.50$ s. The system is controlled with the parameter $R_a = 21.65\Omega$, $R_b = 17.32\Omega$, $R_c = 8.66\Omega$ and $L_c = 10mH$. Figure 21g shows that the instantaneous load voltage of microgrid becomes imbalanced due to the presence of unbalanced load which is controlled by the damping controller that ensures the desired output. Similar results are also obtained using integral LQG, combined PI and model predictive controller.

8.2.3 Performance against three phase unknown load conditions

This section presents the performance of damping controller against unknown load in three phase microgrid [82]. The load voltage varies with the variation of unknown load. The unknown load is added after $t = 0.30$ s with microgrid that changes load parameter values. Thus, the instantaneous voltage of three phase microgrid is changed. The result shown in Fig. 21i verifies that the damping controller provides the desirable performance against unknown load. Integral LQG, combined PI and model predictive controller also provides the similar results that ensure the high performance of these controller.

9 Future challenges in microgrid

The number of microgrid integration in the low-voltage (LV) distribution system is increasing rapidly [106, 135]. The future LV microgrid will require special protection due to the different characteristics of the distribution systems. During the operation, islanded microgrid will face many challenges with increased number of DG [14]. A

large number of DG units will be integrated with the microgrid to fulfil the demand of electricity. Thus, the power balancing, communication between DG units, protection of the microgrid will become a challenge. DG units are interfaced with the microgrid by converter. This has limited fault current feeding capability. Thus, the fuse protection of LV microgrid in the future will become a common challenge. The challenges are related with the protection zone, operation speed of LV microgrid. The converter must be designed properly having the future-ride-through (FRT) requirements. Special energy storage system such as super-capacitor may be used for the FRT protection to control the voltage rise during faults. A large amount of mismatch will be produce between generation units and loads. This mismatch will produce by connecting and disconnecting of microgrid having large number of DG units at the same time. This will produce voltage and frequency fluctuation.

10 Conclusion

This paper presents the use of renewable energy sources and production methods of electricity. The future world will largely depend on the use of renewable energy sources to maintain the daily need for electricity. The importance of microgrid in the present as well as in the future world is described in this paper. The problems related to microgrid and integration challenges of DG units are described in this paper. The increasing number of DG units becomes a common challenge to maintain the operation of microgrid. Many control methods are investigated to control the voltage of islanded microgrid against different scenarios. The control methods ensure reliable and high performance of the operation of islanded microgrid. Table 3 exhibits the comparison between different controllers. It ensures that the overcomes of other controllers are overcome by ILQG controller. The statistics of the energy production from different renewable energy sources are the evidence of the popularity of microgrid throughout the world. The future world will largely depend on microgrid.

Authors' contributions

FRB: Contribution in the collection of all the material, integration the system and control system. PD: Contribution to write, review and edit the paper to improve the quality of English written. SKS: Contribution in the control system. SKD: Supervised the works. All authors read and approved the final manuscript.

Competing interests

The authors declare that they have no competing interests.

Author details

¹Department of Mechatronics Engineering, Rajshahi University of Engineering and Technology, Kajla Rajshahi-6204, Bangladesh. ²School of Information Technology and Mathematical Sciences, University of South Australia, Adelaide, Australia.

Received: 13 July 2018 Accepted: 22 March 2019

Published online: 25 April 2019

Table 3 Comparisons between the Controllers

Name of the controller	Advantages	Limitations
Integral LQG controller	High band width as well as gain and phase margin	-
PID controller	Low order transfer function matrices and easy to implement	Low band width
Model predictive controller	Incorporate the constraint and less effected by noise	Lack of flexibility and high maintenance cost
Damping controller	Low order transfer function matrices and no need to advanced digital signal processing	Critical need for a cost-effective control strategy

References

1. Council, N.R., et al. (2010). *Electricity From Renewable Resources: Status, Prospects, and Impediments*. National Academies Press.
2. Bayindir, R., Hossain, E., Kbalci, E., Perez, R. (2014). A Comprehensive Study on Microgrid Technology. *International Journal of Renewable Energy Research*, 4(4), 1094–1107.
3. De Vries, B.J., Van Vuuren, D.P., Hoogwijk, M.M. (2007). Renewable Energy Sources: Their Global Potential for the First-Half of the 21st Century at a Global Level: An Integrated Approach. *Energy Policy*, 35(4), 2590–2610.
4. Lund, H., & Mathiesen, B.V. (2009). Energy System Analysis of 100% Renewable Energy Systems—The Case of Denmark in Years 2030 and 2050. *Energy*, 34(5), 524–531.
5. Jacobsson, S., & Bergek, A. (2004). Transforming The Energy Sector: The Evolution of Technological Systems in Renewable Energy Technology. *Industrial and Corporate Change*, 13(5), 815–849.
6. Johansson, T.B., & Burnham, L. (1993). *Renewable Energy: Sources for Fuels and Electricity*. Island press.
7. Panwar, N., Kaushik, S., Kothari, S. (2011). Role of Renewable Energy Sources in Environmental Protection: a Review. *Renewable and Sustainable Energy Reviews*, 15(3), 1513–1524.
8. (2017). Renewable capacity statistics. *Tech. Rep.*
9. Pérez-Lombard, L., Ortiz, J., Pout, C. (2008). A Review on Buildings Energy Consumption Information. *Energy and Buildings*, 40(3), 394–398.
10. Carley, S. (2009). State Renewable Energy Electricity Policies: An Empirical Evaluation of Effectiveness. *Energy Policy*, 37(8), 3071–3081.
11. Berndes, G., Hoogwijk, M., Van den Broek, R. (2003). The Contribution of Biomass in the Future Global Energy Supply: a Review of 17 Studies. *Biomass and Bioenergy*, 25(1), 1–28.
12. Liu, Y., Meliopoulos, A., Sun, L., Choi, S. (2018). Protection and Control of Microgrids Using Dynamic State Estimation. *Protection and Control of Modern Power Systems*, 3(1), 31.
13. Jacobson, M.Z., & Delucchi, M.A. (2011). Providing All Global Energy with Wind, Water, and Solar Power, Part I: Technologies, Energy Resources, Quantities and Areas of Infrastructure, and Materials. *Energy Policy*, 39(3), 1154–1169.
14. Liserre, M., Sauter, T., Hung, J.Y. (2010). Future Energy Systems: Integrating Renewable Energy Sources into the Smart Power Grid Through Industrial Electronics. *IEEE Industrial Electronics Magazine*, 4(1), 18–37.
15. Mariam, L., Basu, M., Conlon, M.F. (2016). Microgrid: Architecture, Policy and Future Trends. *Renewable and Sustainable Energy Reviews*, 64, 477–489.
16. Mathiesen, B.V., Lund, H., Karlsson, K. (2011). 100% Renewable Energy Systems, Climate Mitigation and Economic Growth. *Applied Energy*, 88(2), 488–501.
17. Apergis, N., & Payne, J.E. (2010). Renewable Energy Consumption and Economic Growth: Evidence from a Panel of OECD Countries. *Energy Policy*, 38(1), 656–660.
18. Kojabadi, H.M., Chang, L., Boutot, T. (2004). Development of a Novel Wind Turbine Simulator for Wind Energy Conversion Systems Using an Inverter-Controlled Induction Motor. *IEEE Transactions on Energy Conversion*, 19(3), 547–552.
19. Nema, P., Nema, R., Rangnekar, S. (2009). A current and Future State of Art Development of Hybrid Energy System Using Wind and PV-Solar: A Review. *Renewable and Sustainable Energy Reviews*, 13(8), 2096–2103.
20. Slootweg, J., De Haan, S., Polinder, H., Kling, W. (2003). General Model for Representing Variable Speed Wind Turbines in Power System Dynamics Simulations. *IEEE Transactions on Power Systems*, 18(1), 144–151.
21. Martinez, J. (2007). *Modelling and Control of Wind Turbines*. London: Imperial College.
22. Ramakrishnan, V., & Srivatsa, S. (2007). Mathematical Modeling of Wind Energy Systems. *Asian Journal of Information Technology*, 6(11), 1160–1166.
23. Fan, Z.M. (2012). *Mathematical Modelling of Grid Connected Fixed-Pitch Variable-Speed Permanent Magnet Synchronous Generators for Wind Turbines*. Ph.D. dissertation, University of Central Lancashire.
24. Manyonge, A.W., Ochieng, R., Onyango, F., Shichikha, J. (2012). Mathematical Modelling of Wind Turbine in a Wind Energy Conversion System: Power Coefficient Analysis. *Applied Mathematical Sciences*, 6(91), 4527–4536.
25. Jafarzadeh, M., Sipaut, C.S., Dayou, J., Mansa, R.F. (2016). Recent Progresses in Solar Cells: Insight Into Hollow Micro/Nano-Structures. *Renewable and Sustainable Energy Reviews*, 64, 543–568.
26. Apergis, N., & Payne, J.E. (2012). Renewable and Non-Renewable Energy Consumption-Growth Nexus: Evidence from a Panel Error Correction Model. *Energy Economics*, 34(3), 733–738.
27. Parida, B., Iniyar, S., Goic, R. (2011). A Review of Solar Photovoltaic Technologies. *Renewable and Sustainable Energy Reviews*, 15(3), 1625–1636.
28. Maghami, M.R., Hizam, H., Gomes, C., Radzi, M.A., Rezadad, M.I., Hajighorbani, S. (2016). Power Loss Due to Soiling on Solar Panel: A Review. *Renewable and Sustainable Energy Reviews*, 59, 1307–1316.
29. Kannan, N., & Vakeesan, D. (2016). Solar Energy for Future World: A Review. *Renewable and Sustainable Energy Reviews*, 62, 1092–1105.
30. Urban, F., Geall, S., Wang, Y. (2016). Solar PV and Solar Water Heaters in China: Different Pathways to Low Carbon Energy. *Renewable and Sustainable Energy Reviews*, 64, 531–542.
31. Patel, M.R. (2005). *Wind and Solar Power Systems: Design, Analysis, and Operation*. CRC press.
32. OĞUR, O. Concentrated Solar Power Systems. https://en.wikipedia.org/wiki/Concentrated_solar_power.
33. El Gharbi, N., Derbal, H., Bouaichaoui, S., Said, N. (2011). A Comparative Study Between Parabolic Trough Collector and Linear Fresnel Reflector Technologies. *Energy Procedia*, 6, 565–572.
34. Mills, D.R., & Morrison, G.L. (2000). Compact Linear Fresnel Reflector Solar Thermal Powerplants. *Solar Energy*, 68(3), 263–283.
35. Natsheh, E.M., Albarbar, A., Yazdani, J. (2011). Modeling and Control for Smart Grid Integration of Solar/Wind Energy Conversion System, In *Innovative Smart Grid Technologies (ISGT Europe), 2011 2nd, IEEE PES International Conference and Exhibition on* (pp. 1–8). IEEE.
36. Kong, K.C., Mamat, M.B., Ibrahim, M.Z., Muzathik, A. (2012). New Approach on Mathematical Modeling of Photovoltaic Solar Panel. *Applied Mathematical Sciences*, 6(8), 381–401.
37. Ben-Iwo, J., Manovic, V., Longhurst, P. (2016). Biomass Resources and Biofuels Potential for the Production of Transportation Fuels in Nigeria. *Renewable and Sustainable Energy Reviews*, 63, 172–192.
38. Halder, P., Paul, N., Beg, M. (2014). Assessment of Biomass Energy Resources and Related Technologies Practice in Bangladesh. *Renewable and Sustainable Energy Reviews*, 39, 444–460.
39. McKendry, P. (2002). Energy Production from Biomass (part 1): Overview of Biomass. *Bioresource Technology*, 83(1), 37–46.
40. Johnstone, N., Hašćić, I., Popp, D. (2010). Renewable Energy Policies and Technological Innovation: Evidence Based on Patent Counts. *Environmental and Resource Economics*, 45(1), 133–155.
41. Bhattacharya, M., Paramati, S.R., Ozturk, I., Bhattacharya, S. (2016). The Effect of Renewable Energy Consumption on Economic Growth: Evidence from Top 38 Countries. *Applied Energy*, 162, 733–741.
42. Yen, H.-W., & Brune, D.E. (2007). Anaerobic Co-Digestion of Algal Sludge and Waste Paper to Produce Methane. *Bioresource Technology*, 98(1), 130–134.
43. Appels, L., Lauwers, J., Degève, J., Helsen, L., Lievens, B., Willems, K., Van Impe, J., Dewil, R. (2011). Anaerobic Digestion in Global Bio-Energy Production: Potential and Research Challenges. *Renewable and Sustainable Energy Reviews*, 15(9), 4295–4301.
44. Weiland, P. (2010). Biogas Production: Current State and Perspectives. *Applied Microbiology and Biotechnology*, 85(4), 849–860.
45. Demirel, B., & Scherer, P. (2008). The Roles of Acetotrophic and Hydrogenotrophic Methanogens During Anaerobic Conversion of Biomass to Methane: a Review. *Reviews in Environmental Science and Bio/Technology*, 7(2), 173–190.
46. Chynoweth, D.P., Owens, J.M., Legrand, R. (2001). Renewable Methane from Anaerobic Digestion of Biomass. *Renewable Energy*, 22(1), 1–8.
47. Amon, T., Amon, B., Kryvoruchko, V., Zollitsch, W., Mayer, K., Gruber, L. (2007). Biogas Production from Maize and Dairy Cattle Manure—Influence of Biomass Composition on the Methane Yield. *Agriculture, Ecosystems & Environment*, 118(1), 173–182.
48. Bhutta, M.M.A., Hayat, N., Farooq, A.U., Ali, Z., Jamil, S.R., Hussain, Z. (2012). Vertical Axis Wind Turbine—A Review of Various Configurations and Design Techniques. *Renewable and Sustainable Energy Reviews*, 16(4), 1926–1939.
49. Müller, G., Jentsch, M.F., Stoddart, E. (2009). Vertical Axis Resistance Type Wind Turbines for Use in Buildings. *Renewable Energy*, 34(5), 1407–1412.
50. Rose, J.D., & Hiskens, I.A. (2007). Challenges of Integrating Large Amounts of Wind Power, In *Systems Conference, 2007 1st Annual, IEEE* (pp. 1–7). IEEE.

51. Papathanassiou, S.A., & Papadopoulos, M.P. (2001). Mechanical Stresses in Fixed-Speed Wind Turbines Due to Network Disturbances. *IEEE Transactions on Energy Conversion*, 16(4), 361–367.
52. Pena, R., Clare, J., Asher, G. (1996). Doubly Fed Induction Generator Using Back-to-Back PWM Converters and Its Application to Variable-Speed Wind-Energy Generation. *IEE Proceedings-Electric Power Applications*, 143(3), 231–241.
53. Muller, S., Deicke, M., De Doncker, R.W. (2002). Doubly Fed Induction Generator Systems for Wind Turbines. *IEEE Industry Applications Magazine*, 8(3), 26–33.
54. Alsumiri, M., Li, L., Jiang, L., Tang, W. (2018). Residue Theorem Based Soft Sliding Mode Control for Wind Power Generation Systems. *Protection and Control of Modern Power Systems*, 3(1), 24.
55. Miller, A., Muljadi, E., Zinger, D.S. (1997). A Variable Speed Wind Turbine Power Control. *IEEE Transactions on Energy Conversion*, 12(2), 181–186.
56. Grätzel, M. (2004). Conversion of Sunlight to Electric Power by Nanocrystalline Dye-Sensitized Solar Cells. *Journal of Photochemistry and Photobiology A: Chemistry*, 164(1), 3–14.
57. Green, M.A. (1982). Solar Cells: Operating Principles, Technology, and System Applications. <https://www.osti.gov/biblio/6051511-solar-cells-operating-principles-technology-system-applications>.
58. Fahrenbruch, A., & Bube, R. (2012). *Fundamentals of Solar Cells: Photovoltaic Solar Energy Conversion*. Elsevier.
59. Walker, G., et al. (2001). Evaluating MPPT Converter Topologies Using a MATLAB PV model. *Journal of Electrical & Electronics Engineering*, 21(1), 49–56.
60. De Soto, W., Klein, S., Beckman, W. (2006). Improvement and Validation of a Model for Photovoltaic Array Performance. *Solar Energy*, 80(1), 78–88.
61. Salman, S., Xin, A., Zhouyang, W. (2018). Design of a P-&O Algorithm Based MPPT Charge Controller for a Stand-alone 200W PV System. *Protection and Control of Modern Power Systems*, 3(1), 25.
62. Wang, L., Weller, C.L., Jones, D.D., Hanna, M.A. (2008). Contemporary Issues in Thermal Gasification of Biomass and Its Application to Electricity and Fuel Production. *Biomass and Bioenergy*, 32(7), 573–581.
63. Faaij, A., Van Ree, R., Waldheim, L., Olsson, E., Oudhuis, A., Van Wijk, A., Daey-Ouwens, C., Turkenburg, W. (1997). Gasification of Biomass Wastes and Residues for Electricity Production. *Biomass and Bioenergy*, 12(6), 387–407.
64. Lopes, J.P., Hatzigiorgianni, N., Mutale, J., Djapic, P., Jenkins, N. (2007). Integrating Distributed Generation into Electric Power Systems: A Review of Drivers, Challenges and Opportunities. *Electric Power Systems Research*, 77(9), 1189–1203.
65. Bird, L., Milligan, M., Lew, D. (2013). *Integrating Variable Renewable Energy: Challenges and Solutions*.
66. Steen, D., Goop, J., Göransson, L., Nursbo, S., Brolin, M. (2014). *Challenges of Integrating Solar and Wind into The Electricity Grid*, (pp. 95–100).
67. Edris, A.-A. (2012). Opportunities and Challenges of Integrating Wind, Solar and Other Distributed Generation & Energy Storage: Effects on and Values for the Grid, In *Power and Energy Society General Meeting, 2012, IEEE* (pp. 1–4). IEEE.
68. Tchakoua, P., Wamkeue, R., Ouhrouche, M., Slaoui-Hasnaoui, F., Tameghe, T.A., Ekemb, G. (2014). Wind Turbine Condition Monitoring: State-of-the-Art Review, New Trends, and Future Challenges. *Energies*, 7(4), 2595–2630.
69. Asadullah, M. (2014). Barriers of Commercial Power Generation Using Biomass Gasification Gas: a Review. *Renewable and Sustainable Energy Reviews*, 29, 201–215.
70. Levin, D.B., Pitt, L., Love, M. (2004). Biohydrogen Production: Prospects and Limitations to Practical Application. *International Journal of Hydrogen Energy*, 29(2), 173–185.
71. Shafiullah, G., Oo, A.M., Ali, A.S., Wolfs, P. (2013). Potential Challenges of Integrating Large-Scale Wind Energy into The Power Grid—A Review. *Renewable and Sustainable Energy Reviews*, 20, 306–321.
72. Blaabjerg, F., Teodorescu, R., Liserre, M., Timbus, A.V. (2006). Overview of Control and Grid Synchronization for Distributed Power Generation Systems. *IEEE Transactions on Industrial Electronics*, 53(5), 1398–1409.
73. Liserre, M., Blaabjerg, F., Teodorescu, R., Chen, Z. (2004). Power Converters and Control of Renewable Energy Systems, In *ICPE*.
74. Carrasco, J.M., Franquelo, L.G., Bialasiewicz, J.T., Galván, E., PortilloGuisado, R.C., Prats, M.M., León, J.I., Moreno-Alfonso, N. (2006). Power-Electronic Systems for the Grid Integration of Renewable Energy Sources: A Survey. *IEEE Transactions on Industrial Electronics*, 53(4), 1002–1016.
75. Mahmoud, M.S., Hussain, S.A., Abido, M.A. (2014). Modeling and Control of Microgrid: An Overview. *Journal of the Franklin Institute*, 351(5), 2822–2859.
76. Mongkoltanatas, J., Riu, D., LePivert, X (2013). H-Infinity Controller Design for Primary Frequency Control of Energy Storage in Islanding MicroGrid, In *Power Electronics and Applications (EPE), 2013 15th European Conference on* (pp. 1–11). IEEE.
77. Zhong, Q.-C., & Hornik, T. (2013). Cascaded Current-Voltage Control to Improve the Power Quality for a Grid-Connected Inverter with a Local Load. *IEEE Transactions on Industrial Electronics*, 60(4), 1344–1355.
78. Karimi, H., Davison, E.J., Iravani, R. (2010). Multivariable Servomechanism Controller for Autonomous Operation of a Distributed Generation Unit: Design and Performance Evaluation. *IEEE Transactions on Power Systems*, 25(2), 853–865.
79. Bidram, A., Davoudi, A., Lewis, F.L., Guerrero, J.M. (2013). Distributed Cooperative Secondary Control of Microgrids Using Feedback Linearization. *IEEE Transactions on Power Systems*, 28(3), 3462–3470.
80. Mahmud, M.A., Pota, H., Hossain, M. (2012). Full-order Nonlinear Observer-Based Excitation Controller Design for Interconnected Power Systems via Exact Linearization Approach. *International Journal of Electrical Power & Energy Systems*, 41(1), 54–62.
81. Sarkar, S.K., Roni, M.H.K., Datta, D., Das, S.K., Pota, H.R. (2018). Improved Design of High-Performance Controller for Voltage Control of Islanded Microgrid. *IEEE Systems Journal*, 99, 1–10.
82. Babazadeh, M., & Karimi, H. (2013). A robust Two-Degree-of-Freedom Control Strategy for an Islanded Microgrid. *IEEE Transactions on Power Delivery*, 28(3), 1339–1347.
83. Simpson-Porco, J.W., Dörfler, F., Bullo, F. (2017). Voltage Stabilization in Microgrids Via Quadratic Droop Control. *IEEE Transactions on Automatic Control*, 62(3), 1239–1253.
84. Kroposki, B., Lasseter, R., Ise, T., Morozumi, S., Papatliassiou, S., Hatzigiorgianni, N. (2008). Making Microgrids Work. *IEEE Power and Energy Magazine*, 6(3), 40–53.
85. Nikkhajoei, H., & Lasseter, R.H. (2009). Distributed Generation Interface to the CERTS Microgrid. *IEEE Transactions on Power Delivery*, 24(3), 1598–1608.
86. Bevrani, H., & Shokoohi, S. (2013). An Intelligent Droop Control for Simultaneous Voltage and Frequency Regulation in Islanded Microgrids. *IEEE Transactions on Smart Grid*, 4(3), 1505–1513.
87. Bouzid, A.M., Guerrero, J.M., Cheriti, A., Bouhamida, M., Sicard, P., Benghanem, M. (2015). A Survey on Control of Electric Power Distributed Generation Systems for Microgrid Applications. *Renewable and Sustainable Energy Reviews*, 44, 751–766.
88. Lasseter, R., Akhil, A., Marnay, C., Stephens, J., Dagle, J., Guttromson, R., Meliopoulos, A., Yinger, R., Eto, J. (2002). The CERTS Microgrid Concept. *White paper for Transmission Reliability Program, Office of Power Technologies, US Department of Energy*, 2(3), 30.
89. Llaría, A., Curea, O., Jiménez, J., Camblong, H. (2011). Survey on Microgrids: Unplanned Islanding and Related Inverter Control Techniques. *Renewable Energy*, 36(8), 2052–2061.
90. Zhang, D., Li, J., Hui, D. (2018). Coordinated Control for Voltage Regulation of Distribution Network Voltage Regulation by Distributed Energy Storage Systems. *Protection and Control of Modern Power Systems*, 3(1), 3.
91. Sao, C.K., & Lehn, P.W. (2006). Intentional Islanded Operation of Converter Fed Microgrids, In *Power Engineering Society General Meeting, 2006. IEEE* (pp. 6–11). IEEE.
92. Hamzeh, M., Ghafouri, M., Karimi, H., Sheshyekani, K., Guerrero, J.M. (2016). Power Oscillations Damping in DC Microgrids. *IEEE Transactions on Energy Conversion*, 31(3), 970–980.
93. Magdy, G., Mohamed, E.A., Shabib, G., Elbaset, A.A., Mitani, Y. (2018). Microgrid Dynamic Security Considering High Penetration of Renewable Energy. *Protection and Control of Modern Power Systems*, 3(1), 23.
94. Vandoorn, T.L., Renders, B., Degroote, L., Meersman, B., Vandeveldel, L. (2010). Voltage Control in Islanded Microgrids by Means of a Linear-Quadratic Regulator, In *Proc. IEEE Benelux Young Researchers Symposium in Electrical Power Engineering (YRS'10)*. Belgium: Leuven.
95. Pawelek, R., Wasiak, I., Gburczyk, P., Mienski, R. (2010). Study on Operation of Energy Storage in Electrical Power Microgrid-Modeling and Simulation, In *Harmonics and Quality of Power (ICHQP), 2010 14th International Conference on* (pp. 1–5). IEEE.

96. Vasquez, J.C., Guerrero, J.M., Savaghebi, M., Eloy-Garcia, J., Teodorescu, R. (2013). Modeling, Analysis, and Design of Stationary-Reference-Frame Droop-Controlled Parallel Three-Phase Voltage Source Inverters. *IEEE Transactions on Industrial Electronics*, 60(4), 1271–1280.
97. Li, Y.W., Vilathgamuwa, D.M., Loh, P.C. (2006). A Grid-Interfacing Power Quality Compensator for Three-Phase Three-Wire Microgrid Applications. *IEEE Transactions on Power Electronics*, 21(4), 1021–1031.
98. Olivares, D.E., Mehrizi-Sani, A., Etemadi, A.H., Cañizares, C.A., Iravani, R., Kazerani, M., Hajimiragha, A.H., Gomis-Bellmunt, O., Saeedifard, M., Palma-Behnke, R., et al. (2014). Trends in Microgrid Control. *IEEE Transactions on Smart Grid*, 5(4), 1905–1919.
99. Tsikalakis, A.G., & Hatziargyriou, N.D. (2011). Centralized Control for Optimizing Microgrids Operation, In *Power and Energy Society General Meeting, 2011 IEEE* (pp. 1–8). IEEE.
100. Rafa, A.H. (2013). Centralized Controller for Microgrid. *World Academy of Science, Engineering and Technology, International Journal of Electrical, Computer, Energetic, Electronic and Communication Engineering*, 7(9), 1237–1247.
101. Guo, W., & Mu, L. (2016). Control Principles of Micro-source Inverters Used in Microgrid. *Protection and Control of Modern Power Systems*, 1(1), 5.
102. Hatziargyriou, N.D., Dimeas, A., Tsikalakis, A.G., Lopes, J.P., Karniotakis, G., Oyarzabal, J. (2005). Management of Microgrids in Market Environment, In *Future Power Systems, 2005 International Conference on* (pp. 177–193). IEEE.
103. Meng, L., Savaghebi, M., Andrade, F., Vasquez, J.C., Guerrero, J.M., Graells, M. (2015). Microgrid Central Controller Development and Hierarchical Control Implementation in the Intelligent Microgrid Lab of Aalborg University, In *Applied Power Electronics Conference and Exposition (APEC), 2015 IEEE* (pp. 2585–2592). IEEE.
104. Golsorkhi, M.S., & Lu, D.D.-C. (2016). A Decentralized Control Method for Islanded Microgrids Under Unbalanced Conditions. *IEEE Transactions on Power Delivery*, 31(3), 1112–1121.
105. Katiraei, F., Iravani, R., Hatziargyriou, N., Dimeas, A. (2008). Microgrids Management. *IEEE Power and Energy Magazine*, 6(3).
106. Zamora, R., & Srivastava, A.K. (2010). Controls for Microgrids with Storage: Review, Challenges, and Research Needs. *Renewable and Sustainable Energy Reviews*, 14(7), 2009–2018.
107. De Gennaro, M.C., & Jadbabaie, A. (2006). Decentralized Control of Connectivity for Multi-Agent Systems, In *Decision and Control, 2006 45th, IEEE Conference on* (pp. 3628–3633). IEEE.
108. Vasquez Quintero, J.C. (2009). *Decentralized Control Techniques Applied to Electric Power Distributed Generation in Microgrids*. Universitat Politècnica de Catalunya.
109. Hwang, C.-S., Kim, E.-S., Kim, Y.-S. (2016). A Decentralized Control Method for Distributed Generations in an Islanded DC Microgrid Considering Voltage Drop Compensation and Durable State of Charge. *Energies*, 9(12), 1070.
110. Haider, S., Li, G., Wang, K. (2018). A Dual Control Strategy for Power Sharing Improvement in Islanded Mode of AC Microgrid. *Protection and Control of Modern Power Systems*, 3, 1–8.
111. Karimi, H., Nikkhajoei, H., Iravani, R. (2008). Control of an Electronically-Coupled Distributed Resource Unit Subsequent to an Islanding Event. *IEEE Transactions on Power Delivery*, 23(1), 493–501.
112. Katiraei, F., Iravani, M.R., Lehn, P.W. (2005). Micro-Grid Autonomous Operation During and Subsequent to Islanding Process. *IEEE Transactions on Power Delivery*, 20(1), 248–257.
113. Karimi, H., Yazdani, A., Iravani, R. (2008). Negative-Sequence Current Injection for Fast Islanding Detection of a Distributed Resource Unit. *IEEE Transactions on Power Electronics*, 23(1), 298–307.
114. Gao, F., & Iravani, M.R. (2008). A Control Strategy for a Distributed Generation Unit in Grid-Connected and Autonomous Modes of Operation. *IEEE Transactions on Power Delivery*, 23(2), 850–859.
115. Guerrero, J.M., Chandorkar, M., Lee, T.-L., Loh, P.C. (2013). Advanced Control Architectures for Intelligent Microgrids—Part I: Decentralized and Hierarchical Control. *IEEE Transactions on Industrial Electronics*, 60(4), 1254–1262.
116. Vasquez, J.C., Guerrero, J.M., Miret, J., Castilla, M., De Vicuna, L.G. (2010). Hierarchical Control of Intelligent Microgrids. *IEEE Industrial Electronics Magazine*, 4(4), 23–29.
117. Bidram, A., & Davoudi, A. (2012). Hierarchical Structure of Microgrids Control System. *IEEE Transactions on Smart Grid*, 3(4), 1963–1976.
118. Palizban, O., & Kauhaniemi, K. (2015). Hierarchical Control Structure in Microgrids with Distributed Generation: Island and Grid-Connected Mode. *Renewable and Sustainable Energy Reviews*, 44, 797–813.
119. Savaghebi, M., Jalilian, A., Vasquez, J.C., Guerrero, J.M. (2012). Secondary Control Scheme for Voltage Unbalance Compensation in an Islanded Droop-Controlled Microgrid. *IEEE Transactions on Smart Grid*, 3(2), 797–807.
120. Firestone, R., & Marnay, C. (2005). *Energy Manager Design for Microgrids*: Lawrence Berkeley National Laboratory.
121. Marinescu, B., & Bourles, H. (1999). Robust Predictive Control for the Flexible Coordinated Secondary Voltage Control of Large-Scale Power Systems. *IEEE Transactions on Power Systems*, 14(4), 1262–1268.
122. Teodorescu, R., Blaabjerg, F., Liserre, M., Loh, P.C. (2006). Proportional-Resonant Controllers and Filters for Grid-Connected Voltage-Source Converters. *IEE Proceedings-Electric Power Applications*, 153(5), 750–762.
123. Jiang, Z., & Yu, X. (2008). Hybrid DC-and AC-Linked Microgrids: Towards Integration of Distributed Energy Resources, In *Energy 2030 Conference, 2008. ENERGY 2008. IEEE* (pp. 1–8). IEEE.
124. Dannehl, J., Liserre, M., Fuchs, F.W. (2011). Filter-Based Active Damping of Voltage Source Converters with **LCL** Filter. *IEEE Transactions on Industrial Electronics*, 58(8), 3623–3633.
125. Halevi, Y. (1994). Stable LQG Controllers. *IEEE Transactions on Automatic Control*, 39(10), 2104–2106.
126. Rahman, M., Sarkar, S.K., Das, S.K., Miao, Y. (2017). A comparative study of lqr, lqg, and integral lqg controller for frequency control of interconnected smart grid, In *Electrical Information and Communication Technology (EICT), 2017 3rd International Conference on* (pp. 1–6). IEEE.
127. Sikder, S.H., Rahman, M.M., Sarkar, S.K., Das, S.K. (2018). Fractional order robust pid controller design for voltage control of islanded microgrid, In *4th International Conference on Electrical Engineering and Information & Communication Technology (iCEEICT)* (pp. 1–6). IEEE.
128. Sarkar, S.K., Badal, F.R., Das, S.K. (2017). A Comparative Study of High Performance Robust PID Controller for Grid Voltage Control of Islanded Microgrid. *International Journal of Dynamics and Control*, 6, 1–11.
129. Rana, M., Pota, H., Petersen, I.R. (2013). High-Speed AFM Image Scanning Using Observer-Based MPC-Notch Control. *IEEE Transactions on Nanotechnology*, 12(2), 246–254.
130. Sarkar, S.K., Badal, F.R., Das, S.K., Miao, Y. (2017). Discrete Time Model Predictive Controller Design for Voltage Control of an Islanded Microgrid, In *2017 3rd International Conference on Electrical Information and Communication Technology (EICT)* (pp. 1–6). IEEE.
131. Mishra, S., & Ramasubramanian, D. (2015). Improving the Small Signal Stability of a PV-DE-Dynamic load-Based Microgrid Using an Auxiliary Signal in the PV Control Loop. *IEEE Transactions on Power Systems*, 30(1), 166–176.
132. Pogaku, N., Prodanovic, M., Green, T.C. (2007). Modeling, Analysis and Testing of Autonomous Operation of an Inverter-Based Microgrid. *IEEE Transactions on Power Electronics*, 22(2), 613–625.
133. Lasseter, R.H., & Paigi, P. (2004). Microgrid: A Conceptual Solution, In *Power Electronics Specialists Conference, 2004. PESC 04. 2004 IEEE 35th Annual, vol. 6* (pp. 4285–4290). IEEE.
134. Zhou, N., Chi, Y., Wang, Q. (2011). Control Strategies for Microgrid Containing Non-Linear and Unbalanced Loads. *Dianli Xitong Zidonghua(Automation of Electric Power Systems)*, 35(9), 61–66.
135. Laaksonen, H.J. (2010). Protection Principles for Future Microgrids. *IEEE Transactions on Power Electronics*, 25(12), 2910–2918.